EMVA Standard 1288

Standard for Characterization of Image Sensors and Cameras

Release 4.0 General
16 June 2021

Issued by
European Machine Vision Association
www.emva.org

Preface

This document describes Release 4.0 General of the EMVA standard 1288 hosted by the European Machine Vision Association (EMVA). This release supersedes Release 3.1 [9], entered into force on December 30, 2016. The EMVA 1288 standard is endorsed by the G3, an initiative for global coordination of machine vision standards.[1] As it is the case with all G3 standards, this document is publicly available free of charge.

Rights, Trademarks, and Licenses

The EMVA holds the intellectual property of the EMVA 1288 standard[2] and owns the "EMVA, standard 1288 compliant" logo. Any company or institution can obtain a license to use the "EMVA standard 1288 compliant" logo, free of charge, with product specifications measured and presented according to the definitions in EMVA standard 1288.

The licensee guarantees that he meets the terms of use in the relevant release of EMVA standard 1288. Licensed users will self-certify compliance of their measurement setup, computation and representation with which the "EMVA standard 1288 compliant" logo is used. The licensee has to check regularly compliance with the relevant release of EMVA standard 1288. For further details, especially the disclosure of any Intellectual Property right claims

[1] Coorperation agreement on global coordination of machine vision standards, signed on November 3, 2009. Current G3 members include the Automated Imaging Association (AIA), the Chinese Machine Vision Unit (CMVU), the EMVA, the Japanese Industrial Imaging Association (JIIA), and the Mechanical Engineering Industry Association (VDMA).

[2] G3 agreement, §1 preamble, section "Intellectual property"

under control of the licensee with respect to EMVA standard 1288, and how to apply for a license please visit the web page of the EMVA at `https://www.emva.org/` in the standards menu.

Anybody publishing data claimed to be EMVA standard 1288 compliant or provides them to a customer or any third party also has to provide the *full datasheet*.[3] An EMVA 1288 compliant datasheet must contain all mandatory measurements and graphs (Table 1) and the standardized EMVA 1288 summary datasheet (see Section 10.2).

EMVA will not be liable for specifications not compliant with the standard and damage resulting therefrom. EMVA keeps the right to withdraw the granted license if a licensee violates one the license rules.

About this Standard

EMVA has started the initiative to define a unified method to measure, compute and present specification parameters and characterization data for cameras and image sensors used for machine vision applications. The standard does not define what nature of data should be disclosed. It is up to the publisher of the datasheet to decide if he wishes to publish typical data, data of an individual component, guaranteed data, or even guaranteed performance over life time of the component. However it shall clearly be indicated what the nature of the presented data is.

The standard includes *mandatory* measurements which must be performed and reported in the datasheet to be EMVA1288 compliant. Further there are *optional* sections which may be skipped for a component where the respective data is not relevant or applicable. It may be necessary to indicate additional, component specific information, not defined in the standard, to better describe the performance of image sensor or camera products, or to describe properties not covered by the standard. It is possible in accordance with the EMVA1288 standard to include such data in the same datasheet. However the data obtained by procedures not described in the current release must be clearly marked as extra measurements not included in the EMVA 1288 standard.

The standard is intended to provide a concise definition and clear description of the measurement process and to benefit the vision industry by providing fast, comprehensive and consistent access to specification information for cameras and sensors. It will be particularly beneficial for those who wish to compare cameras or who wish to calculate system performance based on the performance specifications of an image sensor or a camera.

Starting with Release 4, the EMVA 1288 standard includes two separate documents. The separte document describes *Release 4 Linear* and is a direct successor of *Release 3.1* [9] with a few changes and extensions. Release 4 Linear, as the name says, is limited to cameras and image sensors with a linear characteristic curve. Together with the photon transfer curve, the basic mean parameters temporal dark noise, system gain and quantum efficiencies can be determined.

This document *Release 4 General* can be used for much wider classes of cameras and image sensors. It no longer relies on a linear characteristic curve or that raw data are provided. The photon transfer curve is no longer used. The essential point is that basically the same measurements are performed, but they are analyzed in a different way providing still all important application relevant parameters.

While the previous releases of the standard focused on monochrome cameras with a single channel and additionally only included color cameras, Release 4 takes into account the significant advance of multimodal imaging, including polarization, multispectral and time-of-flight (depth imaging). Each of these multimodal sensors includes multiple channels. If the raw data from these channels is available, each channel can be characterized with EMVA 1288 measurements. Polarization imaging serves as a model how the rich tool set of the standard can also be applied to parameters, computed from several channels, here the degree of polarization and the angle of (partially) polarized light.

[3] Either online, on request or in justified exceptions, e. g., for an engineering sample or a product in development, with an NDA. This is a question of research integrity. Results must be recorded in such a way that they “allow verification and replication by others” (Singapore Statement on Research Integrity, 2010, `https://wcrif.org/guidance/singapore-statement`

Acknowledgements

EMVA 1288 is an initiative driven by the industry and living from the personal initiative of the supporting companies' and institutions' delegates as well as from the support of these organizations. Thanks to this generosity the presented document can be provided free of charge to the users of this standard. EMVA thanks those contributors (see Appendix E) in the name of the whole vision community.

Contents

1 Introduction and Scope

This release of the standard covers cameras which cannot be handled with Release 4.0 Linear including non-linear cameras and cameras with internal preprocessing changing the temporal noise. It is valid for area scan and line scan cameras. Analog cameras can be described according to this standard in conjunction with a frame grabber; similarly, image sensors can be described as part of a camera. If not specified otherwise, the term camera is used for all these items.

1.1 Structure of Document

The standard text is parted into four sections describing the mathematical model and parameters that characterize cameras and sensors with respect to

- Section 2: sensitivity and noise,
- Section 3: dark current,
- Section 4: sensor array nonuniformities and defect pixels characterization,

a section with an overview of the required measuring setup (Section 5), and five sections that detail the requirements for the measuring setup and the evaluation methods for

- Section 6: sensitivity and noise,
- Section 7: dark current,
- Section 8: sensor array nonuniformities and defect pixels characterization,
- Section 9: spectral sensitivity,

The detailed setup is not regulated in order not to hinder progress and the ingenuity of the implementers. It is, however, mandatory that the measuring setups meet the properties specified by the standard. Section 10 finally describes how to produce the EMVA 1288 datasheets.

Appendix B describes the notation, Appendix D differences in the measurements and parameter evaluation between the the linear and general model followed by the list of contributors in Appendix E and a template of the summary datasheet (Appendix F).

1.2 General Assumptions

It is important to note that Release 4 general can only be applied if the camera under test can actually be described by the general model on which it is based. If these conditions are not fulfilled, the computed parameters are meaningless with respect to the camera under test and thus the standard cannot be applied. The general assumptions include

1. The amount of photons collected by a pixel depends on the irradiance $E(t)$ (units $\mathrm{W/m^2}$) integrated over the exposure time t_{exp} (units s), i. e., the irradiation

$$H = \int_0^{t_{\mathrm{exp}}} E(t)\,\mathrm{d}t \qquad (1)$$

at the sensor plane.

2. The exposure or integration time must be known, but a linear characteristic curve is not required.
3. The temporal noise at one pixel must not be statistically independent from the noise at all other pixels. However, the temporal noise in one image is statistically independent from the noise in the next image. The parameters describing the noise are invariant with respect to time and space. All this implies that the temporal power spectrum of the noise is flat only in time (“white noise”). Preprocessing can takes place. Typical examples include debayering, denoising, and edge sharpening.
4. Temporal noise includes all types of unkown noise sources in the camera and photon shot noise. Therefore Release 4 General can also be applied to intensified and electron multiplying cameras (EM CCD, [3, 4]).
5. Only the total quantum efficiency is wavelength dependent. The effects caused by light of different wavelengths can be linearly superimposed.
6. One photon can generate more than one charge unit. Therefore cameras can be measured using Release 4 General in the deep ultraviolet, where more than one electron per absorbed photon is generated [12].
7. Only the dark current is temperature dependent.

These assumptions describe the properties of an *ideal* camera or sensor. A real sensor will depart more or less from an ideal sensor. As long as the deviation is small, the description is still valid and it is one of the tasks of the standard to describe the degree of deviation from an ideal behavior. However, if the deviation is too large, the parameters derived may be too uncertain or may even be rendered meaningless. Then the camera cannot be characterized using Release 4 General.

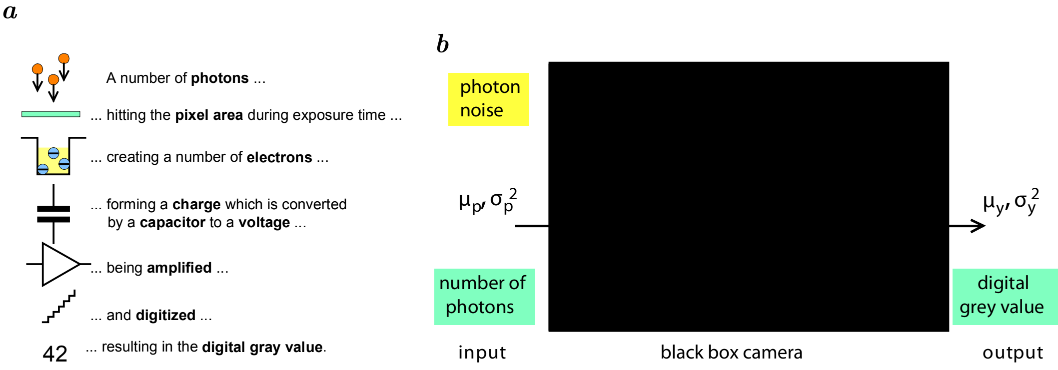

Figure 1: ***a*** *Physical model of the camera and* ***b*** *black box model of a general camera or image sensor. Figures separated by comma represent the mean and variance of a quantity.*

2 Sensitivity and Noise

This section describes how to characterize the sensitivity, linearity, and temporal noise of an image sensor or camera [5, 10, 11, 13].

2.1 Black Box Model

As illustrated in Fig. 1a, a digital image sensor essentially converts photons hitting the pixel area during the exposure time, into a digital number by a sequence of steps. During the exposure time on average μ_p photons hit the whole area A of a single pixel. A fraction

$$\eta(\lambda) = \frac{\mu_e}{\mu_p} \tag{2}$$

of them, the *total quantum efficiency*, is absorbed and accumulates μ_e charge units.[4] The total quantum efficiency as defined here refers to the total area occupied by a single sensor element (pixel) not only the light sensitive area. Consequently, this definition includes the effects of fill factor and microlenses. As expressed in Eq. (2), the quantum efficiency depends on the wavelength of the photons irradiating the pixel.

The mean number of photons that hit a pixel with the area A during the exposure time t_{exp} can be computed from the irradiance E on the sensor surface in W/m^2 by

$$\mu_p = \frac{AEt_{\text{exp}}}{h\nu} = \frac{AEt_{\text{exp}}}{hc/\lambda}, \tag{3}$$

using the well-known quantization of the energy of electromagnetic radiation in units of $h\nu$. With the values for the speed of light $c = 2.99792458 \cdot 10^8$ m/s and Planck's constant $h = 6.6260755 \cdot 10^{-34}$ Js, the photon irradiance is given in handy units for image sensors by

$$\mu_p[\text{photons}] = 50.34 \cdot A[\mu\text{m}^2] \cdot t_{\text{exp}}[\text{ms}] \cdot \lambda[\mu\text{m}] \cdot E\left[\frac{\mu\text{W}}{\text{cm}^2}\right]. \tag{4}$$

This equation is used to convert the irradiance calibrated by radiometers in units of W/cm^2 into photon fluxes required to characterize imaging sensors.

In the camera electronics, the charge units accumulated by the photo irradiance is converted into a voltage, amplified, and finally converted into a digital signal y by an analog digital converter (ADC). In contrast to Release 4 Linear, no assumption is made that the system is linear. On the contrary, nothing is known what happens insight the camera. The model is a true black box. All what is known is that a mean number of photons μ_p with the variance σ_p^2 hit a pixel with known size within a known exposure or integration time,

[4] The actual mechanism is different for CMOS sensors, however, the mathematical model for CMOS is the same as for CCD sensors

resulting in a digital output signal with a mean μ_y and a variance σ_y^2. Still it is possible to measure the input/output relation, the *characteristic curve*

$$\mu_y - \mu_{y.\mathrm{dark}} = R(\mu_p), \tag{5}$$

which in general will be a nonlinear function. Note that the dark value $\mu_{y.\mathrm{dark}}$ is subtracted. Thus the characteristic curve shows the photo-induced signal as a function of the quantum exposure.

Because it is not known what happens in the camera, it is not possible to include any parameters such as the quantum efficiency η or a camera system gain K into the relation for the characteristic curve, as this is the case with a linear camera model for Release 4 Linear. It is also not possible to establish a noise model for the camera. All what is known is that already the input signal if noisy. The number of photons hitting a pixel during the exposure time fluctuates statistically. According to the laws of quantum mechanics, the probability is Poisson distributed. Therefore the variance of the fluctuations is equal to the mean number of photons:

$$\sigma_{p.\mathrm{shot}}^2 = \mu_p. \tag{6}$$

This noise, often referred to as *shot noise* is given by the basic laws of physics and equal for all types of cameras.

2.2 Output and Input Signal-to-Noise Ratio (SNR)

Generally, the quality of the signal is expressed by the signal-to-noise ratio (SNR). The essential part of the general black-box EMVA 1288 approach is based on the fact that the the output signal-to-noise ratio (SNR_y) can be measured directly. With the help of the characteristic curve Eq. (73) it is then possible to infer the input signal-to-noise ratio (SNR_p). Thus the SNR play the key role and it is essential to understand that in a non-linear system input and output SNR are not the same. This is only the case in a linear system.

The SNR of the digital output signal is defined as

$$\mathrm{SNR}_y = \frac{\mu_y - \mu_{y.\mathrm{dark}}}{\sigma_y} \tag{7}$$

and can be measured directly. But it is no direct measure as how sensitive irradiance differences can be measured. In this sense, the output SNR_y is not of relevance. The output standard deviation σ_y with units DN is more important, because it determines whether the output signal is correctly quantized.

The SNR of the input signal, i. e., the number of photons hitting the pixel during the exposure time, is defined as

$$\mathrm{SNR}_p = \frac{\mu_p}{\sigma_p}, \tag{8}$$

where σ_p now does not only include the photon shot noise Eq. (6) but all other noise sources from the in general non-linear processes taking place in the image sensor and the subsequent amplification circuits.

Inverse error propagation can be used to determine the equivalent temporal noise of the input signal form the output signal. The relation between the standard deviation of the output and input signal is determined by the derivative of the characteristic curve

$$\sigma_y = \left|\frac{\partial \mu_y}{\partial \mu_p}\right| \sigma_p. \tag{9}$$

Using this equation and Eqs. (7) and (8), the input SNR is given by

$$\mathrm{SNR}_p = \frac{\mu_p}{\sigma_y}\left|\frac{\partial \mu_y}{\partial \mu_p}\right| = \frac{\mu_p}{\mu_y}\left|\frac{\partial \mu_y}{\partial \mu_p}\right| \mathrm{SNR}_y. \tag{10}$$

For a linear characteristic curve as assumed in Relase 4.0 Linear

$$\mu_y = \eta K \mu_p, \tag{11}$$

input and output SNR are the same:

$$\frac{\partial \mu_y(\mu_p)}{\partial \mu_p} = \eta K \quad \rightsquigarrow \quad \mathrm{SNR}_p = \mathrm{SNR}_y. \tag{12}$$

For a non-linear characteristic curve with a gamma factor γ

$$\mu_y = K_\gamma (\eta \mu_p)^\gamma, \tag{13}$$

input and output SNR

$$\frac{\partial y(\mu_p)}{\partial \mu_p} = K_\gamma(\eta)^\gamma \gamma (\mu_p)^{\gamma-1} \quad \rightsquigarrow \quad \mathrm{SNR}_p = \gamma \mathrm{SNR}_y \tag{14}$$

differ by a factor γ.

A real sensor can always be compared to an *ideal* sensor. An ideal sensor does not add any further noise sources in the black-box model of the camera. The only noise source, the photon shot noise in Eq. (6), comes from the input signal. Thus input signal and input noise are just amplified by the non-linear characteristic curve. The input and output SNR of an ideal sensor are therefore given by

$$\mathrm{SNR}_{p.\mathrm{ideal}} = \sqrt{\mu_p} \quad \text{and} \quad \mathrm{SNR}_{y.\mathrm{ideal}} = \sqrt{\mu_p}\, \frac{\mu_y}{\mu_p} \bigg/ \left| \frac{\partial \mu_y}{\partial \mu_p} \right|. \tag{15}$$

Using this curve in SNR_p graphs, it becomes immediately visible how much lower the SNR_p of a real sensor in comparison to an ideal one. Without any further model, it is, however, not possible to infer why this is the case. In could be a quantum efficiency lower than one, additional noise sources within the nonlinear camera or a combination of both.

2.3 Computation of mean and variance of measured gray values

For the characteristic or sensitivity curve (Section 2.1, Eq. (73)) and the output SNR (Section 2.2, Eq. (7)) it is required to compute the mean gray values and the temporal variance of the gray values at many exposure steps. This is done in an efficient way using only two images taken at the same radiant exposure in the same way as for Release 4.0 Linear:

Mean gray value. The mean of the gray values μ_y over *all* $M \times N$ pixels in the active area at each exposure level is computed from the two captured $M \times N$ images $\boldsymbol{y}[0]$ and $\boldsymbol{y}[1]$ as

$$\mu_y[k] = \frac{1}{NM} \sum_{m=0}^{M-1} \sum_{n=0}^{N-1} y[k][m][n], \ (k = 0, 1) \quad \text{and} \quad \mu_y = \frac{1}{2}(\mu_y[0] + \mu_y[1]) \tag{16}$$

averaging over M rows and N columns.

In the same way, the mean gray value of dark images, $\mu_{y.\mathrm{dark}}$, is computed.

Temporal variance of gray value. Normally, the computation of the temporal variance would require the capture of many images. However on the assumptions put forward in Section 1.2, the temporal noise is stationary and homogenous it could also be averaged over the many pixels of a single image. The variance computed in this way from just one image $\boldsymbol{y}[k]$ contains also the spatial variance of the nonuniformity s_y^2 (see Section 4.2)

$$\frac{1}{NM} \sum_{m=0}^{M-1} \sum_{n=0}^{N-1} (y[k][m][n] - \mu[0])^2 = \sigma_y^2 + s_y^2. \tag{17}$$

Temporal noise causes the gray values to be different from one image to the next, but the nonuniformity is stationary ("fixed pattern noise"). Therefore the variance of spatial nonuniformity can be eliminated by

$$\begin{aligned} \sigma_y^2 &= \frac{1}{2NM} \sum_{m=0}^{M-1} \sum_{n=0}^{N-1} \left[(y[0][m][n] - \mu[0]) - (y[1][m][n] - \mu[1])\right]^2 \\ &= \frac{1}{2NM} \sum_{m=0}^{M-1} \sum_{n=0}^{N-1} (y[0][m][n] - y[1][m][n])^2 - \frac{1}{2} (\mu[0] - \mu[1])^2 . \end{aligned} \tag{18}$$

Because the variance of the difference of two values is the sum of the variances of the two values, the variance of the temporal noise computed in this way must be divided by two as indicated in Eq. (18).
The correction for the variance σ_y^2 in Eq. (18) by the difference of the mean values of the two images is new in Release 4. It gives an unbiased estimate even if the mean values are slightly different by a temporal noise source that causes all pixels to fluctuate in sync.
The statistical uncertainty of the variance estimation averaged over NM values is according to Papoulis [17, Sec. 8.2] and Jähne [13, Sec. 3.4.4] given by

$$\frac{\sigma(\sigma_y^2)}{\sigma_y^2} = \sqrt{\frac{2}{NM}}. \tag{19}$$

This means that for a megapixel image sensor the standard deviation in the estimation of the temporal variance is about 0.14%.[5]

2.4 Signal Saturation and Absolute Sensitivity Threshold

For an k-bit digital camera, the digital gray values are in a range between 0 and $2^k - 1$. The practically useable gray value range is smaller, however. The mean dark gray value $\mu_{y.\mathrm{dark}}$ must be higher than zero so that no significant underflow occurs by temporal noise and the dark signal nonuniformity. Likewise the maximal usable gray value is lower than $2^k - 1$ because of the temporal noise and the photo response nonuniformity.

Therefore, the *saturation irradiation* $\mu_{p.\mathrm{sat}}$ is defined in such a way that the clipping of the distribution is minor so that the computation of both the mean and variance is not biased. For exact definitions see Section 6.5).

From the saturation irradiation $\mu_{p.\mathrm{sat}}$ the *saturation capacity* $\mu_{e.\mathrm{sat}}$ can be computed according to

$$\mu_{e.\mathrm{sat}} = \eta \mu_{p.\mathrm{sat}} \tag{20}$$

only if the quantum efficiency is known, which is not the case for the general model. The same is true for any other derived parameter with units of electrons e^-().

The saturation capacity must not be confused with the *full-well capacity*. It is normally lower than the full-well capacity, because the signal is clipped to the maximum digital value $2^k - 1$ before the physical saturation of the pixel is reached.

The *minimum detectable irradiation* or *absolute sensitivity threshold*, $\mu_{p.\mathrm{min}}$ can be defined by using the input SNR_p. It is the mean number of photons required so that the SNR_p is equal to 1. For this purpose, it is required to interpolate the SNR_p measurements numerically in a suitable way, becasue we do not know an analytical relation as this is the case in Release 4.0 Linear.

The ratio of the signal saturation to the absolute sensitivity threshold is defined as the *dynamic range* (DR):

$$\mathrm{DR} = \frac{\mu_{p.\mathrm{sat}}}{\mu_{p.\mathrm{min}}}. \tag{21}$$

3 Dark Current

3.1 Mean and Variance

The dark signal μ_y.dark is not constant. It is mainly caused by thermally induced electrons. Therefore, the dark signal has an offset of $\mu_{y.0}$ (value at zero exposure time) and increases linearly with the exposure time

$$\mu_{y.\mathrm{dark}} = \mu_{y.0} + \mu_{\mathrm{therm}} = \mu_{y.0} + \mu_{I.y} t_{\mathrm{exp}}. \tag{22}$$

In this equation all quantities are expressed in units DN/pixel. The quantity $\mu_{I.y}$ is named the mean *dark current*, given in the units DN/(pixel s). If a camera or sensor has a dark current compensation, the dark current cannot be characterized using Eq. (22).

[5] Therefore it is also justified to use NM in the estimation of the variance and not the correct value $NM - 1$ for an unbiased estimation. This is just a relative difference of 10^{-6} for a megapixel image sensor.

According to the laws of error propagation, the variance of the dark signal

$$\sigma^2_{y.\mathrm{dark}} = \sigma^2_{y.0} + \sigma^2_{\mathrm{therm}} = \sigma^2_{y.0} + \mu_{I.y} t_{\mathrm{exp}}, \tag{23}$$

should also increase linearly, if it is assumed that within the small change of values caused by the dark current, the characteristic curve is linear.

With the general model it is not possible to compute the dark current in units of electrons. But given the slope of the characteristic curve at the dark value, the mean dark current can be expressed in units of photons, p/(pixel s):

$$\mu_{I.p} = \mu_{I.y} / R_d \ , \tag{24}$$

where the responsivity in the dark, R_d, is the slope of the characteristic curve at zero exposure:

$$R_d = \left. \frac{\partial \mu_y}{\partial \mu_p} \right|_{\mu_p = 0} . \tag{25}$$

3.2 Temperature Dependence

Because of the thermal generation of charge units, the dark current increases roughly exponentially with the temperature [10, 12, 21]. In Release 3.1 this was expressed by

$$\mu_I = \mu_{I.\mathrm{ref}} \cdot 2^{(T - T_{\mathrm{ref}})/T_d}. \tag{26}$$

The constant T_d has units K or ^{o}C and indicates the temperature interval that causes a doubling of the dark current. The temperature T_{ref} is a reference temperature at which all other EMVA 1288 measurements are performed and $\mu_{I.\mathrm{ref}}$ the dark current at the reference temperature. Many modern CMOS sensors no longer show such a simple exponential increase of the dark current. Therefore in Release 4 a specific model about the temperature increase of the dark current is no longer assumed. Only the data are presented.

The measurement of the temperature dependency of the dark current is the only measurement to be performed at different ambient temperatures, because it is the only camera parameter with a *strong* temperature dependence.

4 Spatial Nonuniformity and Defect Pixels

The model discussed so far considered only a single or average pixel. All parameters of an array of pixels, will however vary from pixel to pixel. Sometimes these nonuniformities are called *fixed pattern noise*, or *FPN*. This expression is however misleading, because inhomogeneities are not noise that makes the signal vary in time. The inhomogeneity may only be distributed randomly. Therefore it is better to name this effect *nonuniformity*.

For a linear sensor there are only two basic nonuniformities. The characteristic curve can have a different offset and different slope for each pixel. The dark signal varying from pixel to pixel is called *dark signal nonuniformity*, abbreviated to *DSNU*. The variation of the sensitivity is called *photo response nonuniformity*, abbreviated to *PRNU*. The spatial variations of the dark current, the *dark current nonuniformity*, or *DCNU* and the *full-well capacity* are not yet covered by the EMVA standard 1288.

For a non-linear sensor it is still possible to define the DSNU in the same way, but the PRNU will in general depend on the exposure and is more complex to describe.

4.1 Types of Nonuniformities

Spatial nonuniformities are more difficult to describe than temporal noise because they are not just random. For an adequate description, several effects must be considered:

Gradual variations. Manufacturing imperfections can cause gradual low-frequency variations over the whole chip. This effect is not easy to measure because it requires a very homogeneous irradiation of the chip, which is difficult to achieve. Fortunately this effect does not really degrade the image quality significantly. A human observer does not detect it at all and additional gradual variations are introduced by lenses (shading, vignetting) and nonuniform illumination. Therefore, gradual variations must be corrected with the complete image system anyway for applications that demand a flat response over the whole sensor array.

Periodic variations and spatial patterns. This type of distortion is very nasty, because the human eye detects such distortions very sensitively, especially if there are column and row patterns. Likewise many image processing operations are disturbed.

Outliers. These are single pixels or cluster of pixels that show a significant deviation from the mean.

Random variations. If the spatial nonuniformity is purely random, i. e., shows no spatial correlation, the power spectrum is flat, i. e., the variations are distributed equally over all wave numbers. Such a spectrum is called a *white spectrum*. The outlier pixels also contribute to a flat spectrum.

The EMVA 1288 standard describes nonuniformities in four different ways. The variance of spatial nonuniformity (Section 4.2) and the split into column, row, and pixel variances (Sections 4.3 and 8.2), , introduced in Release 4, are a simple overall measure of the spatial nonuniformity including horizontal and vertical patterns. The spectrogram method, i. e., a power spectrum of the spatial variations (Section 8.6), offers a way to analyze patterns or periodic spatial variations. In the spectrogram, periodic variations show up as sharp peaks with specific spatial frequencies in units cycles/pixel (Section 8.6). The horizontal and vertical profiles (Section 8.7) give a quick direct view of all possible types of nonuniformities. Finally, the characterization of defect pixels by logarithmically scaled histograms (Sections 4.4 and 8.8) is a flexible method to specify unusable or defect pixels according to application specific criteria.

4.2 Spatial Variances

Spatial variances can be computed from just two images taken at the same exposure as the variance of the temporal noise (Section 2.3). Subtracting the terms in Eqs. (17) and (18) yields

$$\begin{aligned} s_y^2 &= \frac{1}{NM}\sum_{m=0}^{M-1}\sum_{n=0}^{N-1}(y[0][m][n]-\mu[0])(y[1][m][n]-\mu[1]) \\ &= \frac{1}{NM}\left(\sum_{m=0}^{M-1}\sum_{n=0}^{N-1}y[0][m][n]y[1][m][n]\right)-\mu[0]\mu[1] \end{aligned} \quad (27)$$

It has been shown theoretically [14] that this expression never becomes negative. This can only happen if the correction for the difference in the two mean values in Eq. (18) would not be applied.

For all other evaluation methods of spatial nonuniformities besides variances, such as histograms, profiles, and spectrograms, it is required to suppress the temporal noise well below the spatial variations. This can only be performed by averaging over a sufficiently large number L of images. In this case, spatial variances are computed in the following way. First a mean image averaged over L images $\boldsymbol{y}[l]$ is computed:

$$\langle \boldsymbol{y} \rangle = \frac{1}{L}\sum_{l=0}^{L-1}\boldsymbol{y}[l]. \quad (28)$$

The averaging is performed over all pixels of a sensor array. The mean value of this image is given by:

$$\mu_y = \frac{1}{MN}\sum_{m=0}^{M-1}\sum_{n=0}^{N-1}\langle y \rangle [m][n], \quad (29)$$

where M and N are the number of rows and columns of the image and m and n the row and column indices of the array, respectively. Likewise, the *spatial variance* s^2 is

$$s^2_{y.\text{measured}} = \frac{1}{MN}\sum_{m=0}^{M-1}\sum_{n=0}^{N-1}(\langle y \rangle [m][n]-\mu_y)^2. \quad (30)$$

All spatial variances are denoted with the symbol s^2 to distinguish them easily from the temporal variances σ^2. The spatial variances computed from L averaged images have to be corrected for the residual variance of the temporal noise. This is why it is required to subtract σ_y^2/L:

$$s^2_{y.\mathrm{stack}} = s^2_{y.\mathrm{measured}} - \sigma_y^2/L. \tag{31}$$

4.3 Column, Row, and Pixel Spatial Variances

Modern CMOS sensors may exhibit not only pixel-to-pixel nonuniformities, but also row-to-row and/or column-to-column nonuniformities. This means that it is important to decompose the spatial variance into row, column, and pixel variances:

$$s_y^2 = s^2_{y.\mathrm{row}} + s^2_{y.\mathrm{col}} + s^2_{y.\mathrm{pixel}}. \tag{32}$$

This decomposition applies also for line-scan cameras with a slightly different meaning. Because in the end any line-scan camera acquires images, row variations are caused by temporal variations from row to row.

With the proposed split of the spatial variances, there are now three unknowns instead of only one unknown. All three unknowns can still be estimated by computing additional spatial variances from a row and column averaged over the whole image.

The variances can be computed for each exposure step from only two images or for a more detailed analysis from an average over many images. Therefore the following equations are written in a general way using a mean image $\langle \boldsymbol{y} \rangle$ according to Eq. (28) averaged over L images. The mean row, mean column, and mean value are then given by

$$\mu_y[n] = \frac{1}{M}\sum_{m=0}^{M-1} \langle y \rangle [m][n], \quad \mu_y[m] = \frac{1}{N}\sum_{n=0}^{N-1} \langle y \rangle [m][n], \quad \mu_y = \frac{1}{MN}\sum_{m=0}^{M-1}\sum_{n=0}^{N-1} \langle y \rangle [m][n]. \tag{33}$$

The *column spatial variance* computed from the average row

$$s^2_{y.\mathrm{col}} = \frac{1}{N}\sum_{n=0}^{N-1} (\mu_y[n] - \mu_y)^2 - s^2_{y.\mathrm{pixel}}/M - \sigma_y^2/(LM) \tag{34}$$

still contains a residual *pixel spatial variance* and temporal variance, because the averaging over M rows does not completely suppress theses variances. Therefore the two terms on the right hand need to be subtracted.

Likewise, the *row spatial variance* computed from the average column

$$s^2_{y.\mathrm{row}} = \frac{1}{M}\sum_{m=0}^{M-1} (\mu_y[m] - \mu_y)^2 - s^2_{y.\mathrm{pixel}}/N - \sigma_y^2/(LN) \tag{35}$$

contains residual *pixel spatial variance* and temporal variance from averaging over N columns, and these also need to be subtracted.

The three equations (32), (34), and (35) form a linear equation system from which all three components of the spatial variance can be computed. With the two abbreviations

$$\begin{aligned} s^2_{y.\mathrm{cav}} &= \frac{1}{N}\sum_{n=0}^{N-1} (\mu_y[n] - \mu_y)^2 \quad - \quad \sigma_y^2/(LM), \\ s^2_{y.\mathrm{rav}} &= \frac{1}{M}\sum_{m=0}^{M-1} (\mu_y[m] - \mu_y)^2 \quad - \quad \sigma_y^2/(LN), \end{aligned} \tag{36}$$

the linear equation system reduces to

$$\begin{bmatrix} 1 & 0 & 1/M \\ 0 & 1 & 1/N \\ 1 & 1 & 1 \end{bmatrix} \begin{bmatrix} s^2_{y.\mathrm{col}} \\ s^2_{y.\mathrm{row}} \\ s^2_{y.\mathrm{pixel}} \end{bmatrix} = \begin{bmatrix} s^2_{y.\mathrm{cav}} \\ s^2_{y.\mathrm{rav}} \\ s^2_y \end{bmatrix}. \tag{37}$$

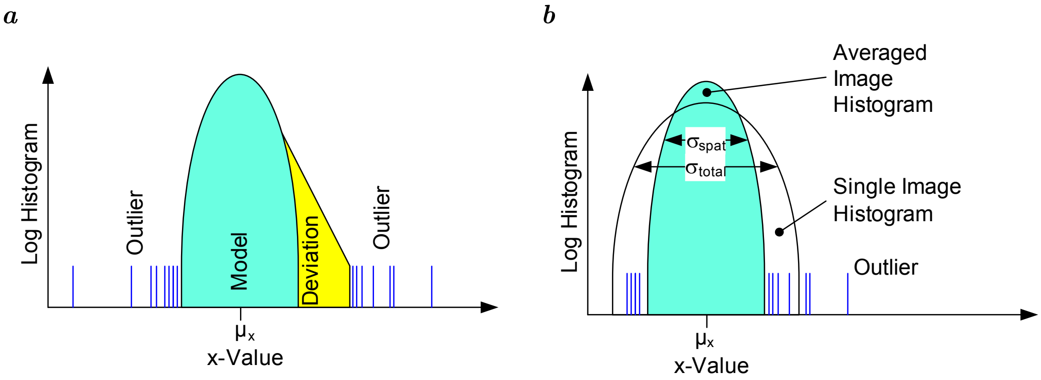

Figure 2: *Logarithmic histogram of spatial variations* ***a*** *Showing comparison of data to model and identification of deviations from the model and of outliers,* ***b*** *Comparison of logarithmic histograms from single images and averaged over many images.*

Solving this linear equation system yields

$$\begin{bmatrix} s^2_{y.\mathrm{col}} \\ s^2_{y.\mathrm{row}} \\ s^2_{y.\mathrm{pixel}} \end{bmatrix} = \frac{1}{MN-M-N} \begin{bmatrix} M(N-1) & N & -N \\ M & N(M-1) & -M \\ -MN & -NM & NM \end{bmatrix} \begin{bmatrix} s^2_{y.\mathrm{cav}} \\ s^2_{y.\mathrm{rav}} \\ s^2_{y} \end{bmatrix} \tag{38}$$

or

$$\begin{aligned} s^2_{y.\mathrm{col}} &= \frac{MN-M}{MN-M-N} s^2_{y.\mathrm{cav}} - \frac{N}{MN-M-N}(s^2_y - s^2_{y.\mathrm{rav}}), \\ s^2_{y.\mathrm{row}} &= \frac{MN-N}{MN-M-N} s^2_{y.\mathrm{rav}} - \frac{M}{MN-M-N}(s^2_y - s^2_{y.\mathrm{cav}}), \\ s^2_{y.\mathrm{pixel}} &= \frac{MN}{MN-M-N}(s^2_y - s^2_{y.\mathrm{cav}} - s^2_{y.\mathrm{rav}}) \end{aligned} \tag{39}$$

For large M and N, the solution simplifies to

$$\begin{aligned} s^2_{y.\mathrm{col}} &\approx s^2_{y.\mathrm{cav}}, \\ s^2_{y.\mathrm{row}} &\approx s^2_{y.\mathrm{rav}}, \\ s^2_{y.\mathrm{pixel}} &\approx s^2_y - s^2_{y.\mathrm{cav}} - s^2_{y.\mathrm{rav}} \end{aligned} \tag{40}$$

This approximative solution is only given for easier understanding, the computations should be performed with the exact solution Eq. (39).

4.4 Defect Pixels

As application requirements differ, it will not be possible to find a common denominator to exactly define when a pixel is defective and when it is not. Therefore it is more appropriate to provide *statistical information* about pixel properties in the form of histograms. In this way anybody can specify how many pixels are unusable or defective using application-specific criteria.

The statistical analysis outlines here is not influenced at all whether the characteristic curve is linear or not. Therefore exactly the same analysis can be performed for Release 4.0 General as for Relese 4.0 Linear.

4.4.1 Logarithmic Histograms It is useful to plot the histograms with logarithmic y-axis for two reasons (Fig. 2a). Firstly, it is easy to compare the measured histograms with a normal distribution, which shows up as a negatively shaped parabola in a logarithmic plot. Thus it is easy to see deviations from normal distributions. Secondly, even single outliers can be distinguished from the many pixels following the normal distribution.

All histograms have to be computed from pixel values that come from averaging over many images. In this way the histograms only reflect the statistics of the spatial noise and

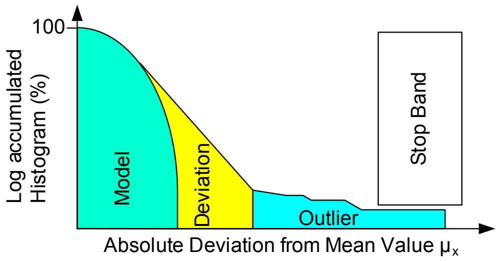

Figure 3: *Accumulated histogram with logarithmic y-axis.*

the temporal noise is averaged out. The statistics from a single image is different. It contains the total noise, i.e. the spatial and the temporal noise.

It is hard to generally predict how far a deviation from the model will impact the final applications. Some of them will have human spectators, while others use a variety of algorithms to make use of the images. While a human spectator is usually able to work well with pictures in which some pixels show odd behaviors, some algorithms may suffer from it. Some applications will require defect-free images, some will tolerate some outliers, while others still have problems with a large number of pixels slightly deviating. All this information can be read out of the logarithmic histograms.

4.4.2 Accumulated Histograms A second type of histogram, the accumulated histogram is useful in addition (Fig. 3). It is computed to determine the ratio of pixels deviating by more than a certain amount. This can easily be connected to the application requirements. Quality criteria from camera or chip manufacturers can easily be drawn in this graph. Usually the criteria is, that only a certain amount of pixels deviates more than a certain threshold. This can be reflected by a rectangular area in the graph. Here it is called *stop band* in analogy to drawings from high-frequency technologies that should be very familiar to electronics engineers.

***Table 1:** List of all EMVA 1288 measurements with classification into mandatory and optional measurements.*

Type of measurement	Mandatory	Reference
Sensitivity, temporal noise and linearity	Y	Section 6
Nonuniformity	Y	Sections 8.2 and 8.6
Defect pixel characterization	Y	Section 8.8
Dark current	Y	Section 7.1
Temperature dependence on dark current	N	Section 7.2
Spectral measurements $\eta(\lambda)$	N	Section 9

5 Overview Measurement Setup and Methods

The characterization according to the EMVA 1288 standard requires three different measuring setups:

1. A setup for the measurement of sensitivity, SNR and nonuniformity using a homogeneous monochromatic light source (Sections 6 and 8).
2. The measurement of the temperature dependency of the dark current requires some means to control the temperature of the camera. The measurement of the dark current at the standard temperature requires no special setup (Section 7).
3. A setup for spectral measurements of the quantum efficiency over the whole range of wavelengths to which the sensor is sensitive (Section 9).

The setup and measurements are basically the same for both the linear and general model. The two approaches differ in some parts of the evaluation of the data.

Each of the following sections describes the measuring setup and details the measuring procedures. All camera settings (besides the variation of exposure time where stated) *must be identical* for all measurements. For different settings (e. g., gain) different sets of measurements must be acquired and different sets of parameters, containing all parameters which may influence the characteristic of the camera, must be presented. Line-scan sensors are treated as if they were area-scan sensors. Acquire at least 100 lines into one image and then proceed as with area-scan cameras for all evaluations except for the computation of vertical spectrograms (Section 8.6).

Not all measurements are mandatory as summarized in Table 1. A data sheet is only EMVA 1288 compliant if the results of *all* mandatory measurements from at least one camera are reported. If optional measurements are reported, these measurements must fully comply to the corresponding EMVA 1288 procedures.

6 Methods for Sensitivity, Linearity, and Noise

6.1 Geometry of Homogeneous Light Source

For the measurement of the sensitivity, linearity and nonuniformity, a setup with a light source is required that irradiates the image sensor homogeneously without a mounted lens. Thus the sensor is illuminated by a diffuse disk-shaped light source with a diameter D placed in front of the camera (Fig. 4a) at a distance d from the sensor plane. Each pixel must receive light from the whole disk under an angle. This can be defined by the *f-number* of the setup, which is is defined as:

$$f_{\#} = \frac{d}{D}. \tag{41}$$

Measurements performed according to the standard require an f-number of 8.

The best available homogeneous light source is an integrating sphere. Therefore it is not required but recommended to use such a light source. But even with a perfect integrating sphere, the homogeneity of the irradiation over the sensor area depends on the diameter of the sensor, D' [15, 16]. For a distance $d = 8 \cdot D$ (f-number 8) and a diameter D' of the image

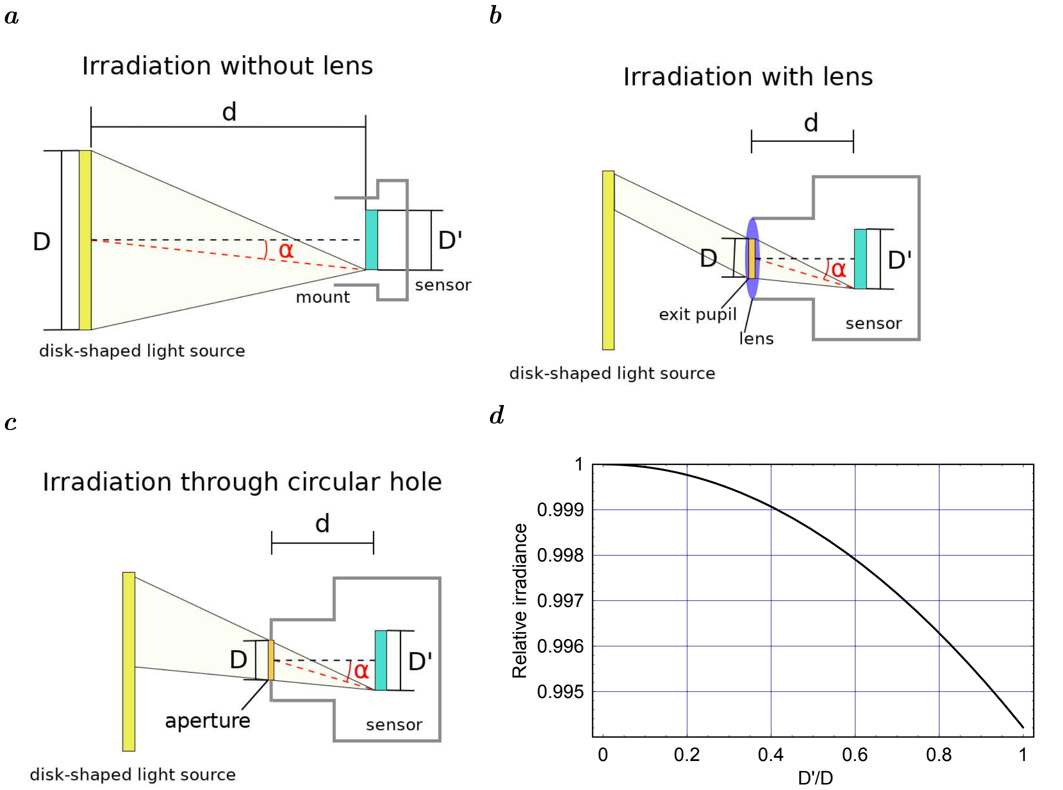

Figure 4: *Optical setup for the irradiation of the image sensor **a** without a lens, **b** with a lens, and **c** through a circular hole by a disk-shaped light source. The dashed red line is the chief ray at the edge of the sensor with an angle α to the optical axis, also denoted as the chief ray angle (CRA). **d** Relative irradiance at the edge of a image sensor with a diameter D', illuminated by a perfect integrating sphere with an opening D at a distance $d = 8D$.*

sensor equal to the diameter of the light source, the decrease is only about 0.5% (Fig. 4d). Therefore the diameter of the sensor area should not be larger than the diameter of the opening of the light source.

A real illumination setup even with an integrating sphere has a much worse inhomogeneity, due to one or more of the following reasons:

Reflections at lens mount. Reflections at the walls of the lens mount can cause significant inhomogeneities, especially if the inner walls of the lens mount are not suitably designed and are not carefully blackened and if the image sensor diameter is close to the free inner diameter of the lens mount.

Anisotropic light source. Depending on the design, a real integrating sphere will show some residual inhomogeneities. This is even more the case for other types of light sources.

Therefore it is essential to specify the spatial nonuniformity of the illumination, ΔE. It should be given as the difference between the maximum and minimum irradiance over the area of the measured image sensor divided by the average irradiance in percent:

$$\Delta E[\%] = \frac{E_{\max} - E_{\min}}{\mu_E} \cdot 100. \tag{42}$$

It is recommended that ΔE is not larger than 3%. This recommendation results from the fact that the linearity should be measured over a range from 5–95% of the full range of the sensor (see Section **??**).

A weak point in the definition of the irradiation geometry of a sensor is that it only specifies the f-number, but not the position of the exit pupil, here simply the distance d to the spherical opening of the light source. For typical EMVA 1288 measuring equipment, the position of the light source is much further away than the exit pupil of lenses. The irradiation conditions are almost as for image-sided telecentric lenses. This can also cause vignetting, for instance, if a full-format image sensor with a 42 mm image circle is used with an F-mount camera. Because of the condition that the diameter D' of the image sensor must be smaller than the diameter D of the light source, the angle α of the chief ray at the edge of the sensor (Fig. 4a) is $\alpha < \arctan(d/2D) \approx 3.6^{\circ}$.

EMVA 1288 measurements will not give useful results if a sensor has microlenses, whose center is shifted away from the center of a pixel towards the edge of the sensor to adapt to the oblique chief ray angle of a lens with short exit pupil distance to the sensor. In this case the irradiation condition described above, will result in a significant fall-off of the signal towards the edge of the sensor.

Therefore with Release 4, optional EMVA 1288 measurements can also be done with camera lens combinations. For a standard measurement, the lens f-number must be set to 8 and focused to infinity. The calibration must also be performed with the lens (for details see Section 6.4). In this case, the camera lens combination looks into a light source (Fig. 4b) which must be homogeneous and isotropic for the whole field angle of the lens. All EMVA 1288 measurements can be performed in this way. It is important to note that the measured PRNU now includes the combined effect of lens and sensor. However, this is very useful to investigate, which camera/lens combination results in the lowest possible fall-off towards the edge. In order to be independent of a specific lens and mimic only the geometry of the irradiation, instead of a lens a circular hole with the exit pupil distance d corresponding to the design chief ray angle (α or CRA) of the image sensor can be used (Fig. 4c). The exit pupil distance d and the diameter of the aperture D are related to the CRA of an image sensor with a diameter D' by

$$d = \frac{D'/2}{\tan\alpha} \quad \text{and} \quad D = \frac{d}{f_\#}. \tag{43}$$

Of course, additional optional measurements can be performed with other f-numbers or a lens focused to a given working distance if this is of importance for a given application. Of special interest are measurements with lower f-numbers, in order to examine to what extent the wide cone of a fast lens is captured by the image sensor.

6.2 Spectral and Polarization Properties of Light Source

The guiding principle for all types of sensors is the same: Choose the type of irradiation that gives the maximum response. In other words, that type for which the corresponding camera channel was designed for. In order to compute the mean number of photons hitting the pixel during the exposure time (μ_p) from the image irradiance E at the sensor plane according to Eq. (4), narrow-band irradiation must be used in all cases. Only then is it possible to perform the measurements without the need to know the spectral response of the camera, which is only an optional measurement (Table 1).

For *gray-scale cameras* it is therefore recommended to use a light source with a center wavelength matching the maximum quantum efficiency of the camera under test. As required by the application, additional measurements with any other wavelength can always be performed. The *full width half maximum* (FWHM) of the light source should be less than 50 nm.

For the measurement of *color cameras* or *multispectral cameras*, the light source must be operated with different wavelength ranges, each wavelength range must be close to the maximum response of one of the corresponding color channels. Normally these are the colors blue, green, and red, but it could be any combination of color channels including channels in the ultraviolet and infrared. For color cameras and multispectral cameras the FWHM should be smaller than the bandwidth of the corresponding channel.

Such light sources can be achieved, e. g., by a light emitting diode (LED) or a broadband light source such as an incandescent lamp or an arc lamp with appropriate bandpass filters. The centroid wavelength λ_c, and the full width half maximum (FWHM) of the light source must be specified. The centroid wavelength of the light source is used for computation of the number of photons according to Eq. (3).

The best approach is to measure these quantities directly using a spectrometer. It is also valid to use the specifications given from the manufacturer of the light source. For a halogen light source with a bandpass filter, a good estimate of the spectral distribution of the light source is given by multiplying the corresponding blackbody curve with the transmission curve of the filter.

The measurement of *polarization cameras* requires light with *linear polarization*. The requirements for the *degree of linear polarization* P (Section **??**) are high. The quantity $1 - P$ should be at least ten times lower than the expected value for the polarizing image sensor. The polarization angle of the light is aligned with the first polarization channel by searching the maximum average response from this channel. For measurements of residual polarization effects with normal cameras, this step is not required.

6.3 Variation of Irradiation

Basically, there are three possibilities to vary the radiant exposure of the sensor, i. e., the radiation energy per area received by the image sensor:

I. Constant illumination with variable exposure time.
With this method, the light source is operated with constant radiance and the radiant exposure is changed by the variation of the exposure time. The radiant exposure H is given as the irradiance E times the exposure time t_{exp} of the camera. Because the dark signal generally may depend on the exposure time, it is required to measure the dark image at *every* exposure time used. The absolute calibration depends on the true exposure time being equal to the exposure time set in the camera.

II. Variable continuous illumination with constant exposure time.
With this method, the radiance of the light source is varied by any technically possible way that is sufficiently reproducible. With LEDs this is simply achieved by changing the current. The radiant exposure H is given as the irradiance E times the exposure time t_{exp} of the camera. Therefore the absolute calibration depends on the true exposure time being equal to the exposure time set in the camera.

III. Pulsed illumination with constant exposure time.
With this method, the radiant exposure of the sensor is varied by the pulse length of the LED. When switched on, a constant current is applied to the LEDs. The radiant exposure H is given as the LED irradiance E times the pulse length t. The sensor exposure time is set to a constant value, which is larger than the maximum pulse length for the LEDs. The LEDs pulses are triggered by the "integrate enable" or "strobe out" signal from the camera. The LED pulse must have a short delay to the start of the integration time and it must be made sure that the pulse fits into the exposure interval so that there are no problems with trigger jittering. The pulsed illumination technique must not be used with rolling shutter mode. Alternatively it is possible to use an external trigger source in order to trigger the sensor exposure and the LED flashes synchronously.

According to basic assumptions number one and two made in Section 1.2, all three methods are equivalent because the amount of photons collected and thus the digital gray value depends only on the product of the irradiance $E(t)$ integrated over the exposure time. Depending on the available equipment and the properties of the camera to be measured, one of the three techniques for irradiation variation or a combination of them can be chosen.

6.4 Calibration of Irradiation

The irradiance must be calibrated absolutely by using a calibrated photodiode put at the place of the image sensor. The calibration accuracy of the photodiode as given by the calibration agency plus possible additional errors related to the measuring setup must be specified together with the data. The accuracy of absolute calibrations are typically between 3% and 5%, depending on the wavelength of the light. The reference photodiode should be recalibrated at least every second year. This will then also be the *minimum systematic error* of the measured quantum efficiency and all related parameters which contain photons in its units.

The radiant exposure H of a pixel with the total area A recieved during the exposure time t_{exp} in units of photons is computed according to Eq. (4). If pixel *binning* is applied, the area of a pixel has to be multiplied by the horzontal and vertical binning factor. Likewise for a *time delay integration* (TDI) sensor, where multiple exposures are accumulated, the exposure time is multiplied by the TDI factor.

For measurements with lens/camera combinations, the same calibration procedures can be applied. Because of the often significant lens shading, it is important that the photodiode is sufficiently small compared to the diameter of the image sensor for a correct calibration in the center of the sensor. A smaller diameter of a photodiode can easily be achieved by placing a pinhole in front of the photodiode. This pinhole must precisely be located in the same distance as the image sensor.

The precision of the calibration of the different irradiance levels must be much higher than the absolute accuracy in order to estimate the characteristic curve and its local slope accurately enough (Sections 2.1 and 6.6). Therefore, the standard deviation of the calibration curve from a linear regression must be lower than 0.1% of the maximum value.

6.5 Measurement Conditions for Characteristic Curve and SNR

Temperature. The measurements are performed at room temperature or a controlled temperature elevated above the room temperature. The type of temperature control must be specified. Measure the temperature of the camera housing by placing a temperature sensor at the lens mount with good thermal contact. If a cooled camera is used, specify the set temperature. Do not start measurements before the camera has come into thermal equilibrium.

Digital resolution. Set the number of bits as high as possible in order to minimize the effects of quantization on the measurements.

Gain. Set the gain of the camera as small as possible without saturating the signal due to the full well capacity of any pixel (this almost never happens). If with this minimal gain, the dark noise $\sigma_{y.\mathrm{dark}}$ is smaller than 0.5 DN, the dark noise cannot be measured reliably. (This happens only in the rare case of a 8-bit camera with a high-quality sensor.) Then only an upper limit for the temporal dark noise can be calculated. The dynamic range is then limited by the quantization noise.

Offset. Set the offset of the camera as small as possible but large enough to ensure that the dark signal including the temporal noise and spatial nonuniformity does not cause any significant underflow. This can be achieved by setting the offset at a digital value so that less than about 0.5% of the pixels underflow, i. e., have the value zero. This limit can easily be checked by computing a histogram and ensures that not more than 0.5% of the pixels are in the bin zero.

Distribution of radiant exposure values. Use at least 50 radiant exposures resulting in digital gray value from the dark gray value and the maximum digital gray value. Only for production measurements as few as 9 suitably chosen values can be taken. For a sensor with a linear or close to linear characteristic curve, the exposure steps can be linear. For non-linear cameras and HDR camera generally more exposure steps must be taken and the exposure should include low saturation in the region where the input SNR is about one.

Number of measurements taken. Capture two images at each exposure level. To avoid transient phenomena when the live grab is started, the two images are taken from a live image series. It is also required to capture two images each without exposure (dark images) at *each* exposure time used for a proper determination of the mean and variance of the dark gray value, which may depend on the exposure time (Section 3).

6.6 Evaluation of the Slope of the Characteristic Curve

Besides the input SNR_p, the characteristic curve plays a central role in the general model. Because in this case no analytical expression of the characteristic curve is given, it is necessary to perform a suitable regression of the characteristic curve with which it is also possible to compute also the first derivative, the slope of the characteristic curve.

This can best be performed by a cubic B-spline regression.This is a very flexible regression method using polynomials of third order within P intervals. In each of the intervals there is a different polynomial of third order. The function value, first and second derivative are continuous at the interval boundaries.

With this approach the characteristic curve is modeled as

$$\mu_y - \mu_{y.\mathrm{dark}} = \sum_{p=0}^{P+2} a_p \beta_3 \left(\frac{\mu_p}{\Delta\mu_p} - (p-1) \right). \tag{44}$$

The exposure range from zero to $\mu_{p.\mathrm{sat}}$ is devided into P intervals of width $\Delta\mu_p = \mu_{p.\mathrm{sat}}/P$. The cubic B-spline function is non-zero only in four intervals

$$\beta_3(x) = \begin{cases} 2/3 - |x|^2 + 1/2|x|^3, & |x| < 1 \\ 1/6(2-|x|)^3, & 1 \le |x| \le 2 \\ 0 & \text{else} \end{cases} \tag{45}$$

and a_p are the $P+3$ regression parameters.

Although this looks complex, it is nothing else than a simple *linear* regression problem with $P+3$ regression parameters, as can be seen from

$$\mu_y(\mu_p) = \sum_{p=0}^{P+3} a_p f_p \quad \text{with basis functions} \quad f_p(\mu_p) = \beta_3 \left(\frac{\mu_p}{\Delta\mu_p} - (p-1) \right). \tag{46}$$

A fast least-squares solution possible with $Q > P+3$ measurement points $\mu_y(\mu_p)$ is possible by

$$\sum_{q=1}^{Q} \left(\sum_{p=0}^{P+3} a_p f_p(\mu_p) - \mu_y(\mu_p) \right)^2 \to \min. \tag{47}$$

Once the regression parameters a_p are computed, also the slope of the regression curve is given by first-order derivation of the characteristic curve, which can now be performed analytically

$$\frac{\partial\mu_y}{\partial\mu_p} = \sum_{p=0}^{P+3} a_p \beta_3' \left(\frac{\mu_p}{\Delta\mu_p} - (p-1) \right) \tag{48}$$

with the derivative of cubic B-spline

$$\beta_3'(x) = \begin{cases} -2x(1 - 3/4|x|), & |x| < 1 \\ x/(2|x|)(2-|x|)^2, & 1 \le |x| \le 2\ . \\ 0 & \text{else} \end{cases} \tag{49}$$

With this approach it is possible to compute the slope of the characteristic curve for each measure exposure value. For the recommended number of exposure steps, 6 to 8 intervals are recommends. For more exposure steps corresondingly more intervals P can be taken.

6.7 Evaluation of Characteristic Curve and Derived Parameters

As described in Section 2, the characteristic curve and the computation of the SNR requires the measurement of the mean gray values and the temporal variance of the gray together with the irradiance per pixel in units photons/pixel. The method to compute the mean and variance are given in Section 2.3.

The measured mean photo-induced gray values $\mu_y - \mu_{y.\mathrm{dark}}$ is shown versus the quantum exposure H in units photons/pixel in the *characteristic curve* (Fig. 5). If the exposure is changed by changing the exposure time (method I in Section 6.3), a second graph must be provided which shows $\mu_{y.\mathrm{dark}}$ as a function of the exposure time t_{exp}.

The temporal standard deviation σ_y according to Eq. (18) and the difference of the mean of the two consecutively captured images, $\mu[0] - \mu[1]$, versus the mean photo-induced gray values $\mu_y - \mu_{y.\mathrm{dark}}$ are shown in the *stability graph* Fig. 6.

The estimation of derived quantities according to the photon transfer method is performed as follows:

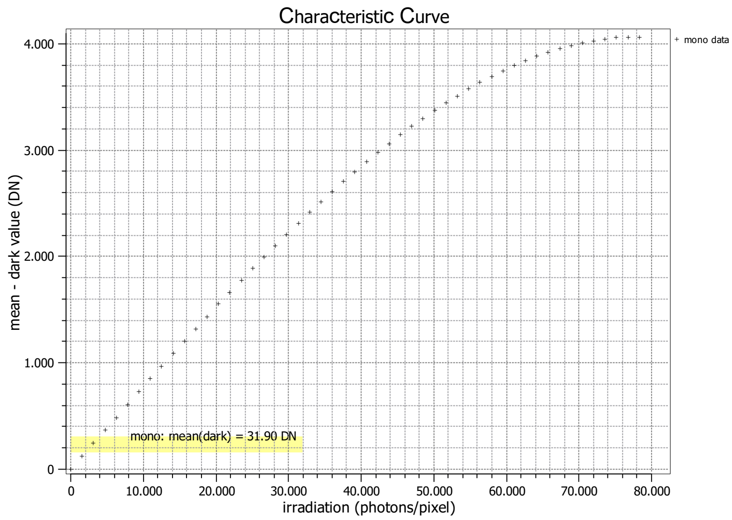

Figure 5: *Example of a nonlinear characteristic curve. The graph draws the measured mean photo-induced gray values* $\mu_y - \mu_{y.dark}$ *versus the radiant exposure* μ_p *in units photons/pixel. The mean dark value is also noted.*

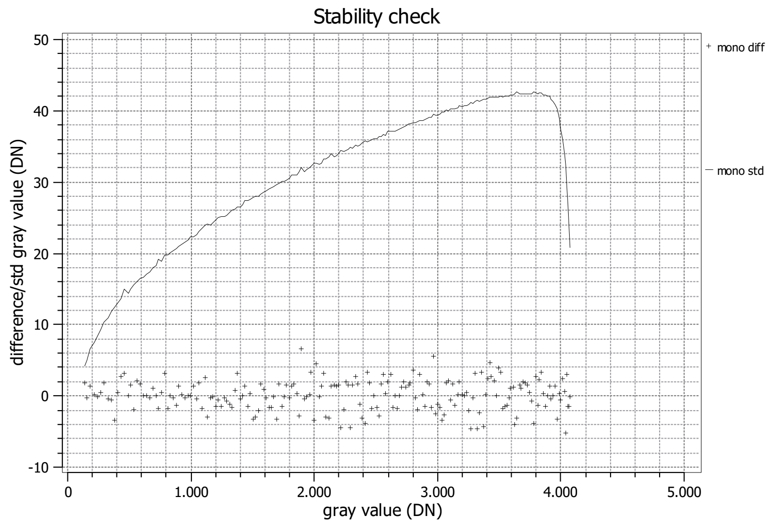

Figure 6: *Example of a stability graph. The graph shows the temporal standard deviation according to Eq. (18) and the difference of the mean of the two consecutively captured images,* $\mu[0] - \mu[1]$*, versus the mean photo-induced gray values* $\mu_y - \mu_{y.dark}$*.*

Saturation. The saturation gray value $\mu_{y.\mathrm{sat}}$ is given as the mean gray value where the histogram of the gray value distribution is not significantly cut-off so that the estimate of the mean value and especially the variance is not biased. With this technique it is required to first find the maximum possible value. For a sensor with a resolution of k bits, this is normally the value $2^k - 1$. But for some sensors, this may be a smaller value. Therefore it is first required to find the maximum possible value y. Then set the exposure by adjusting the exposure time and/or radiance of the light source just as high that between 0.1 - 0.2% of the total number of pixels show the maximum value. With this setting, the bias in the variance estimation is less than 0.37% for a normal distribution. Accumulate the histogram from one or two images without any averaging.

Overall system gain K. With the general model it is not possible to estimate the system gain.

Quantum efficiency η. The quantum efficiency η cannot be measured with the general model. However it is possible to measure the wavelength dependency of the quantum efficiency relative to the wavelength chosen for the other measurements, see Section 9.

Temporal dark noise. It is required to compute two values.

1. For measurement method I with variable exposure time in Section 6.3 the temporal dark noise is found as the offset of the correspondence of the $\sigma^2_{y.\mathrm{dark}}$ over the exposure times. For the measurement method II and III in Section 6.3 make an extra measurement at a minimal exposure time to estimate $\sigma_{y.\mathrm{dark}}$. Use this value to compute the dynamic range. This value gives the actual performance of the camera at the given bit resolution and thus includes the quantization noise.
2. The temporal dark noise cannot be computed in units e^-. This has to be replaced by the dark nosie in units of photons. It is still possible to eliminate the effects of quantization noise. The division by the system gain is replaced by a division by the responsitivity in the dark, R_d, as defined in Eq. (25):

$$\sigma_d = \sqrt{(\sigma^2_{y.\mathrm{dark}} - \sigma^2_q)} \Big/ R_d. \tag{50}$$

If $\sigma^2_{y.\mathrm{dark}} < 0.24$, the temporal noise is dominated by the quantization noise and no reliable estimate is possible (Section C). Then $\sigma_{y.\mathrm{dark}}$ must be set to 0.49 and the upper limit of the temporal dark noise in units p *without* the effects of quantization is given by

$$\sigma_d < \frac{0.40}{R_d}. \tag{51}$$

Absolute sensitivity threshold $\mu_{p.\mathrm{min}}$ is given as the quantum exposure in inits photons required to reach a SNR_p of one. This values has to be estimated by a regression to the SNR_p curve, because there is no analytical expression for SNR_p in the general model (see Section 6.8).

Saturation capacity $\mu_{p.\mathrm{sat}}$. The saturation capacity $\mu_{p.\mathrm{sat}}$ is the number of photons which corresponds to the maximum measured digital value $\mu_{y.\mathrm{sat}}$ as described at the beginning of this section. The saturation capacity $\mu_{e.\mathrm{sat}}$ in e^- cannot be computed.

Dynamic range (DR). Use the definition Eq. (21) in Section 2.4 to compute the dynamic range. It should be given as a ratio and in dB ($20 \log_{10} \mathrm{DR}$).

6.8 Input SNR

The measured mean and the variance of the gray values are used to compute the output SNR_y according to Eq. (7). Then use Eq. (10) to compute the input SNR_p, Eq. (8). These values are plotted in a double logarithmic plot and the SNR curve for an ideal sensor Eq. (15).

Perform a cubic B-spline regression of the inverse SNR relation $\mu_p(\mathrm{SNR}_p)$ over the whole range up to saturation with the same number of intervals as for the characteristic curve and use this regression to compute $\mu_p(\mathrm{SNR}_p = 1)$, which is equal to the absolute sensitivity threshold $\mu_{p.\mathrm{min}}$. If there are discontinuities in the SNR_p curve (e. g., for multilinear sensors) perform the regression only from the lowest value up to the first discontinuity with a correspondingly lower number of intervals.

Search from all calculated SNR_p calue the maximum. This is then the maximum achievable $\mathrm{SNR}_{\mathrm{max}}$. For a linear sensor the maximum SNR_p occurs at the saturation exposure but for a non-linear sensor it could be at a different position. Express this value as a ratio and in dB ($20 \log_{10} \mathrm{SNR}$).

6.9 Evaluation of Multichannel Cameras

For any camera with multiple channels, each channel is evaluated separately. Thus all parameters in the previous section and following sections are computed for each channel with the same equations as for a monochrome camera. In this way it is not only possible to analyze color, multispectral and polarization cameras but also the raw channels of any type of multichannel cameras, provided the raw channel data can be accessed. One possible example are the multiple taps of a time-of-flight depth camera.

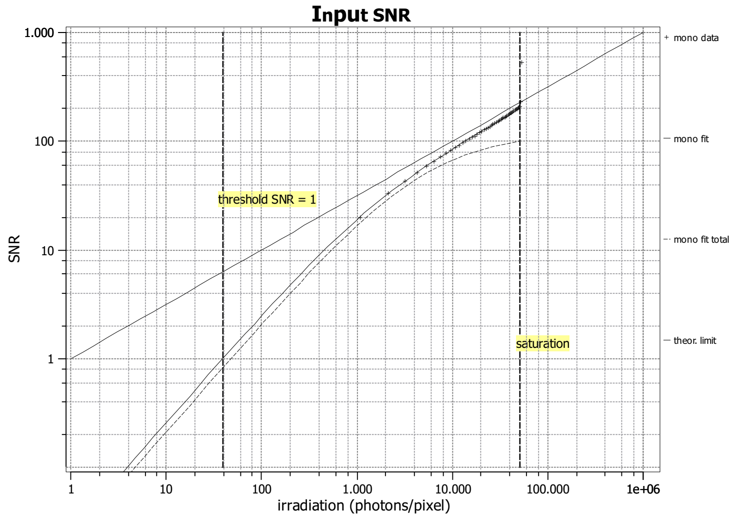

Figure 7: *Example of a input SNR_p graph. It contains the measured SNR and SNR_{total} values and the SNR curve for an ideal sensor Eq. (15). The absolute sensitivity threshold and the saturation capacity are marked by vertical dashed lines.*

6.10 Evaluation of Derived Parameters

For derived quantities, the same methods can be applied to compute mean values and their temporal variance at all exposure steps as for raw data. Compute the derived parameters from the corresponding channels for all pixels from the two images taken at the same exposure *after* subtraction of an averaged dark image as it is used for a detailed analysis of nonuniformity, i. e., use $\boldsymbol{y}_j - \langle \boldsymbol{y}_{j.\mathrm{dark}} \rangle$ for all channels.

Care must only be taken in two cases:

- Parameters that are the ratio of two parameters cannot be computed in the dark, because the parameter is not defined in this case.
- *Circular parameters* such as thehue for a color sensor show a discontinuity from the maximum to the minimum value. In this case an indirect approach must be taken. Circular parameters show an equation of the following type, see document for Release 4.0 Linear:

$$\alpha = \arctan\left(\frac{y}{x}\right), \tag{52}$$

which can be used to compute the mean and variance of α using the laws of error propagation:

$$\mu_\alpha = \arctan\left(\frac{\mu_y}{\mu_x}\right), \quad \sigma_\alpha^2 = \frac{x^2\sigma_y^2 + y^2\sigma_x^2}{(x^2+y^2)^2}. \tag{53}$$

Do not compute the mean of α over all pixels directly from the α values at all pixels, because close to the discontinuity erroneous results will be obtained. Instead it is required to compute the mean and variance from $\boldsymbol{x}$ and $\boldsymbol{y}$.

7 Methods for Dark Current

7.1 Evaluation of Dark Current at One Temperature

Dark current measurements require no illumination source. From Eqs. (22) and (23) in Section 3 it is evident that the dark current can either be measured from the linear increase of the mean or the variance of the dark gray value y_{dark} with the exposure time. The preferred method is, of course, the measurement of the mean, because the mean can be estimated more accurately than the variance. If, however, the camera features a dark current compensation, the dark current must be estimated using the variance.

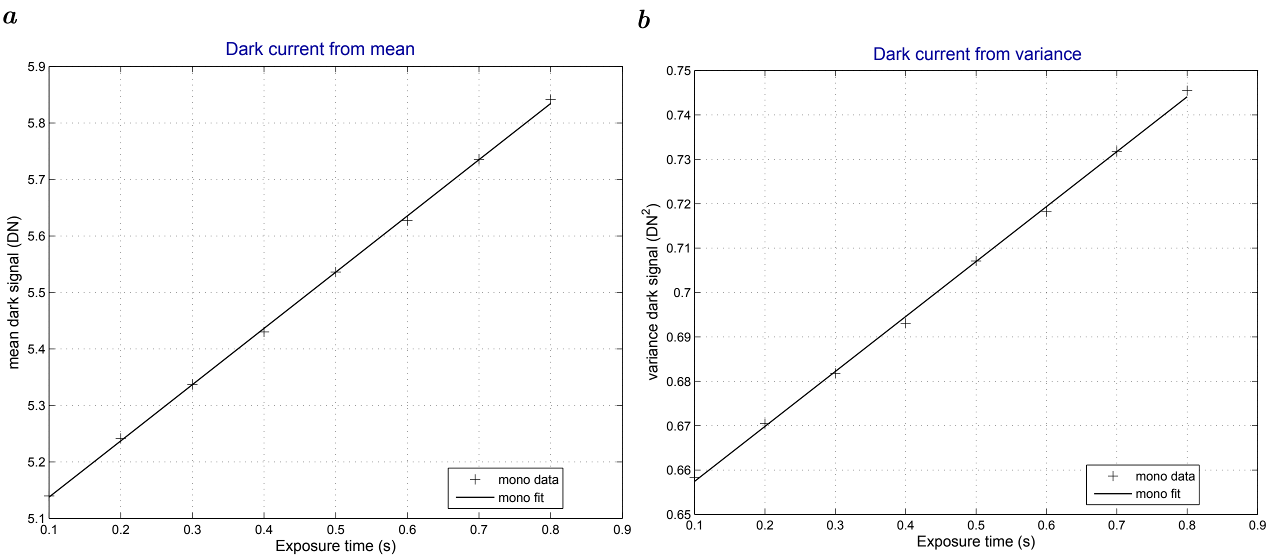

Figure 8: *Examples for dark current measurements: graph of the **a** dark value and **b** temporal variance versus the exposure time. The linear regressions line are also shown.*

At least six equally spaced exposure times must be chosen. It is recommended to choose much longer exposure times than for the sensitivity, linearity, and noise measurements, best to the maximum exposure time recommended by the camera manufacturer.

The dark current is then given as the slope in the relation between the exposure time and mean and variance of the dark value (Fig. 8). A linear least squares regression of the measured dark values gives the dark current in units DN/s and DN^2/s, respectively. Divide the values by the measured slope of the characteristic curve at zero exposure, Eq. (25), R_d and R_d^2, respectively, to obtain the dark current also in units p/s.

If the camera's exposure time is not set long enough to result in meaningful values for the dark current, this value still must be reported together with its one-sigma error from the regression. In this way at least an upper limit of the dark current can be given, provided that $\mu_I + \sigma_I > 0$.

The measured dark current can be used to estimate the standard deviation of the temporal noise at any exposure time t_{any}:

$$\sigma_{y.\text{dark}}(t_{\text{any}}) = \sqrt{\sigma^2_{y.\text{dark}}(t_{\text{exp}}) + \mu_{I.y}(t_{\text{any}} - t_{\text{exp}})} \tag{54}$$

and any other parameter derived from the temporal dark noise. The quantity t_{exp} is the exposure time at which the temporal dark noise was measured (Section 2.3).

7.2 Evaluation of Dark Current at Multiple Temperatures

The temperature dependency of the dark current is determined by measuring the dark current as described above for different housing temperatures. For temperatur measurement see Section 6.5. The temperatures must vary over the whole range of the operating temperature of the camera and should include at least 6 equally spaced temperatures within this range. Put a capped camera in a climate exposure cabinet or control its temperature in another suitable way and drive the housing temperature to the desired value for the next measurement. For cameras with internal temperature regulation and cooling of the image sensor no climate cabinet is required. Then the temperature dependence of the dark current can only be measured in the temperature range that can be set.

After a temperature change wait until the camera values are stable. This is most easily done by continuously measuring the dark values at the largest exposure time. For each temperature, determine the dark current by taking a series of measurements with varying exposure times as described in Section 7.1.

The results of the temperature dependency of the dark current is reported in a dark current (logarithmic scale) versus temperature (linear scale) plot as shown in Fig. 9.

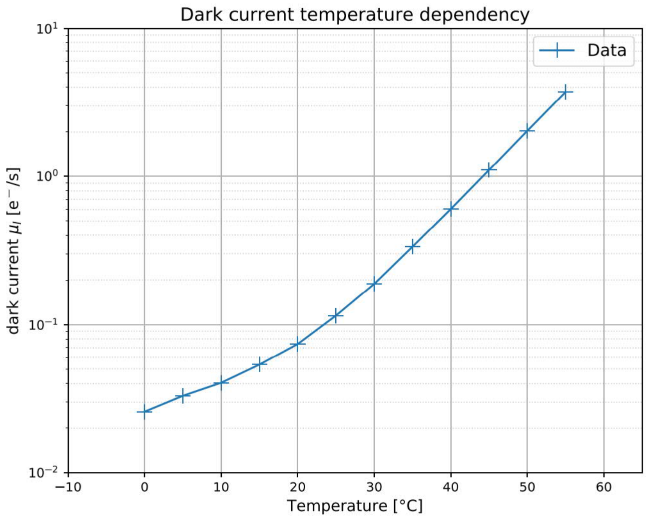

Figure 9: *Example of a measuring curve to determine the dark current temperature dependency. The graph draws the measured dark current μ_I in units e$^-$/s versus the temperature T.*

8 Methods for Spatial Nonuniformity and Defect Pixels

The measurements for spatial nonuniformity and the characterization of defect pixels are performed with the same setup as the sensitivity, linearity, and noise, described in Section 6. Therefore, the basic measuring conditions are also the same (Section 6.5).

All quantities describing nonuniformities, except for the spatial variances (Section 4.2), must be computed from mean gray values averaged over many images. This is because the variance of the temporal noise ($\sigma_y \approx 1\%$) is typically larger than or about the same as the variance of the spatial variations ($s_y \approx 0.3 - 1.0\%$). The temporal noise can only be suppressed by averaging over many images. Typically averaging over L =100–500 images is required.

Because of the general model, it depends on the special type of the sensor, where it is most useful to apply the averaging over a whole sequence. Mandatory choices are for zero exposure (dark images) at 50% saturation for compatibility to Release 4.0 Linear. Additional exposures can be chosen depending on the properties of the sensor.

However, the variances introduced in Section 4.2, and only these, can be computed already with sufficient statistical certainty from only two images and are therefore available for each exposure step. This is also helpful for choosing additional exposure levels for a detailed analysis of spatial nonuniformity.

As for all other evaluations with the general model, the analysis of the nonuniformity parameters is transformed back to the input signal. The key for an easy computation is the observation that the nonuniformities are small compared to the signal range so that the characteristic curve can be linearized:

$$\langle \boldsymbol{p} \rangle = \mu_p(\mu_y) + (\langle \boldsymbol{y} \rangle - \mu_y) \bigg/ \frac{\partial \mu_y(\mu_y)}{\partial \mu_p}, \quad \langle \boldsymbol{p}_d \rangle = (\langle \boldsymbol{y} \rangle - \mu_{y.\mathrm{dark}}) / R_d\,. \tag{55}$$

For zero exposure the mean value in photons is zero.

In the same way all variances computed for the output images in units DN are transformed into variance of the input signal with units photons by using the slope of the characteristic curve using Eq. (9):

$$\sigma_p^2 = \sigma_y^2 \bigg/ \left(\frac{\partial \mu_y}{\partial \mu_p}\right)^2. \tag{56}$$

8.1 Correction for Uneven Illumination

This section addresses the problem that the photoresponse distribution may be dominated by gradual variations in illumination source, especially the typical fall-off of the irradiance towards the edges of the sensor. Low-frequency spatial variations of the image sensor, however, are of less importance, because of two reasons. Firstly, lenses introduce a fall-off towards the edges of an image (*lens shading*). Except for special low-shading lenses, this effect makes a significant contribution to the low-frequency spatial variations. Secondly, almost all image processing operations are not sensitive to gradual gray value changes. (See also discussion in Section 4.1 under item gradual variations.)

In order to show the properties of the camera rather than the properties of an imperfect illumination system, a highpass filter is applied before performing all nonuniformity related computations. In this way the effect of low spatial frequency sensor properties is suppressed. This includes all statistical parameters (Sections 4.2 and 8.3), spectrograms (Section 8.6), and all histograms for defect pixel characterization (Section 8.8). Only for the horizontal and vertical profiles (Section 8.7) no highpass filtering is applied. This means that the profiles show also the large scale nonuniformity but can be biased by an uneven illumination.

For highpass filtering the following two-step filtering is applied. First the images are smoothed by the following filters, one applied after the other: A 7×7 box filter, an 11×11 box filter, and a 3×3 binomial filter. In a second step this smoothed image is subtracted form the original image, leaving only the high-frequency part of the nonuniformities in the resulting image. Theoretical details for this choice of highpass filtering are detailed in Appendix E.3 of the document for Release 4.0 Linear.

8.2 Spatial Standard Deviations

For a detailed analysis of spatial nonuniformity it is also required to compute spatial variances from the stack of L images according to the equations given in Section 4.2. The variance of the temporal noise must be computed directly from the same stack of images $\boldsymbol{y}[l]$ as the mean of the variance at every pixel using

$$\sigma^2_{s[m][n]} = \frac{1}{L-1}\sum_{l=0}^{L-1}\left(y[l][m][n] - \frac{1}{L}\sum_{l=0}^{L-1} y[l][m][n]\right)^2 \quad \text{and} \quad \sigma^2_{y.\text{stack}} = \frac{1}{MN}\sum_{m=0}^{M-1}\sum_{n=0}^{N-1}\sigma^2_{s[m][n]}. \tag{57}$$

8.3 DSNU, and PRNU

The DSNU_{1288} values is given by

$$\text{DSNU}_{1288} = s_{p.\text{dark}} = s_{y.\text{dark}}/R_d \qquad \text{(units p)}. \tag{58}$$

For the PRNU_{1288} it is first required to transform the mean and standard deviations back into the linear input signal. Then the quantity is given by

$$\text{PRNU}_{1288} = \frac{\sqrt{s^2_{p.50} - s^2_{p.\text{dark}}}}{\mu_{p.50}} \qquad \text{(units \%)}. \tag{59}$$

The index 1288 has been added to these definitions because many different definitions of these quantities can be found in the literature. The DSNU_{1288} is expressed in units p and DN. The PRNU_{1288} is defined as a standard deviation relative to the mean value. In this way, the PRNU_{1288} gives the spatial standard deviation of the photoresponse nonuniformity in % from the mean.

All the equations in this section are not only applied to the total spatial variance, but also to the column, row, and pixel variances. The corresponing DSNUs and PRNUs are denoted by $\text{DSNU}_{1288.\text{col}}$, $\text{DSNU}_{1288.\text{row}}$, $\text{DSNU}_{1288.\text{pixel}}$, $\text{PRNU}_{1288.\text{col}}$, $\text{PRNU}_{1288.\text{row}}$, and $\text{PRNU}_{1288.\text{pixel}}$.

8.4 Spatial Standard Deviations of Derived Parameters

In the same way as temporal standard deviations can be computed for parameters derived from more one or more channels (Section 6.10) it is also possible to compute standard deviations of spatial nonuniformities for these quantities.

8.5 Total SNR

The spatial nonuniformities can be included into the SNR resulting in the total SNR. For the general model no analytical expression is available to express both the SNR_p and the total SNR_p. But it is simply possible to add the variances of temporal noise and spatial nonuniformity:

$$\boxed{\mathrm{SNR}_{p.\mathrm{total}}(\mu_p) = \frac{\mu_p}{\sqrt{\sigma_p^2(\mu_p) + s_p^2(\mu_p)}}.} \tag{60}$$

In this way it is possible to include at each exposure step also the total input $\mathrm{SNR}_{p.\mathrm{total}}$ into the SNR plot in Fig. 7. In contrast to the linear model, model curves are not included.

8.6 Horizontal and Vertical Spectrograms

Spectrograms are computed from the DSNU image $\langle \boldsymbol{p}_{\mathrm{dark}} \rangle$ and the PRNU image $\langle \boldsymbol{p}_{50} \rangle$. The computation of the horizontal spectrograms requires the following computing steps:

1. Subtract the mean value from the image $\boldsymbol{y}$.
2. Compute the Fourier transform of each row vector $\boldsymbol{y}[m]$:

$$\hat{p}[m][v] = \frac{1}{\sqrt{N}} \sum_{n=0}^{N-1} p[m][n] \exp\left(-\frac{2\pi i n v}{N}\right) \quad \text{for} \quad 0 \le v < N.. \tag{61}$$

3. Compute the mean power spectrum $p[v]$ averaged over all M row spectra:

$$P[v] = \frac{1}{M} \sum_{m=0}^{M-1} \hat{p}[m][v] \hat{p}^*[m][v], \tag{62}$$

   where the superscript $*$ denotes the complex conjugate. The power spectrum according to Eq. (62) is scaled in such a way that white noise gets a flat spectrum with a mean value corresponding to the spatial variance s_p^2.
   In the spectrograms the square root of the power spectrum, $\sqrt{p[v]}$, is displayed as a function of the spatial frequency v/N (in units of cycles per pixel) up to $v = N/2$ (Nyquist frequency). It is sufficient to draw only the first part of the power spectrum because the power spectrum has an even symmetry

$$P[N - v] = P[v] \quad \forall v \in [1, N/2].$$

   In these plots the level of the white noise corresponds directly to the standard deviation of the spatial white noise. Please note that the peak height in the spectrograms are not equal to the amplitude of corresponding periodic patterns. The amplitude a of a periodic pattern can be computed by adding up the spatial frequencies in the power spectrum belonging to a peak:

$$a = 2\left(\frac{1}{N}\sum_{v_{\min}}^{v_{\max}} P[v]\right)^{1/2}. \tag{63}$$

   For the vertical spectrograms (area cameras only), the same computations are performed (Fig. 10b and Fig. 11b). Only rows and columns must be interchanged.

4. Add a line with the DSNU_{1288} Eq. (58) and PRNU_{1288} Eq. (59) to the corresponding spectrogram plots (Figs. 10 and 11). Because the PRNU is given as a relative value to the mean value (Eq. (59)), also the spectrogram values and the temporal noise (see next item) must be divided by the mean values.
5. Also add a line with the standard deviation of the temporal noise, $\sigma_{y.\mathrm{stack}}$ according to Eq. (57) (Figs. 10 and 11). In this way, it is easy to compare spatial and temporal noise.

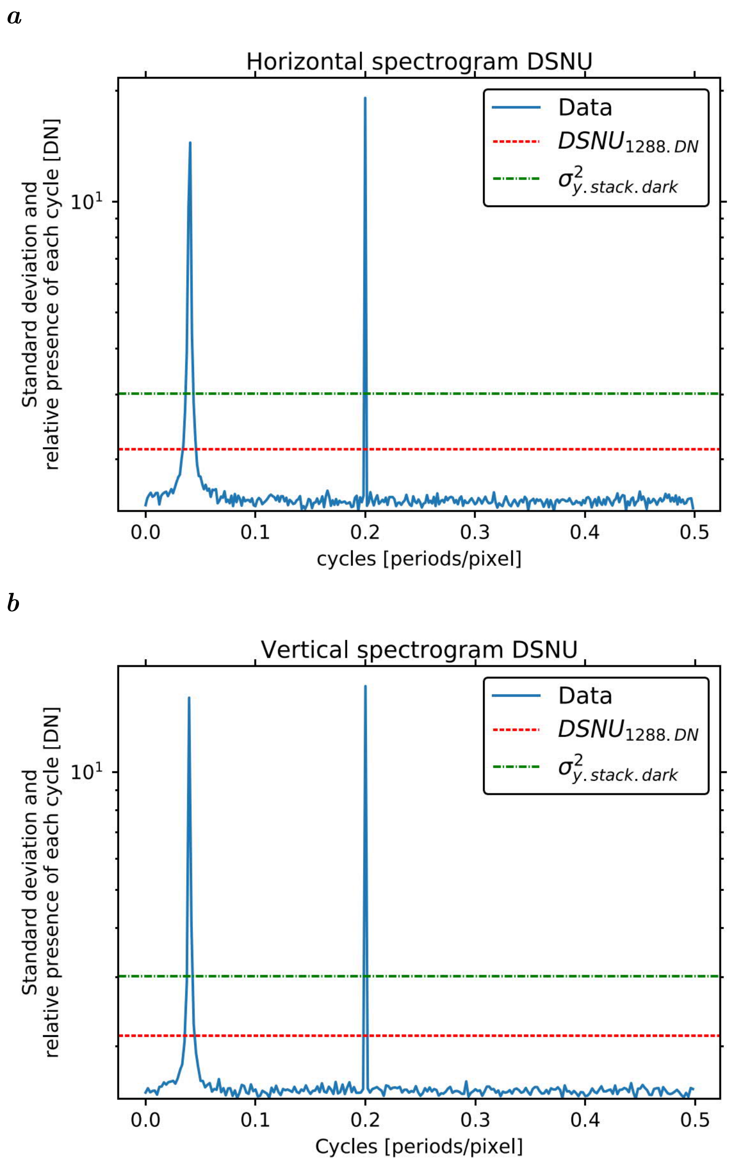

Figure 10: *Example for spectrograms of the dark image:* ***a*** *horizontal spectrogram* ***b*** *vertical spectrogram.*

8.7 Horizontal and Vertical Profiles

The spatial nonuniformities are further illustrated by plots of horizontal and vertical profiles of the DSNU and PRNU — in total four plots. Each plot contains four profiles (Example Fig. 12)

middle: Horizontal row $M/2$ (vertical profile of column $N/2$) through the center of the image. The correct row/column number is given by integer arithmetics, i. e., the largest integer smaller than the half value; indices start with 0.

mean: Average of all rows (all columns).

max: Maximum of all rows (all columns) at each horizontal (vertical) position. These profiles nicely show even only few pixels with positive outliers, e. g. hot pixels in the DSNU image.

min: Minimum of all rows (all columns) at each horizontal (vertical) position. These profiles nicely show even only few pixels with negative outliers, e. g. less sensitive pixels in the PRNU image.

The profiles are directly computed from the averaged dark image $\langle \boldsymbol{y}_{\text{dark}} \rangle$ and the PRNU

a

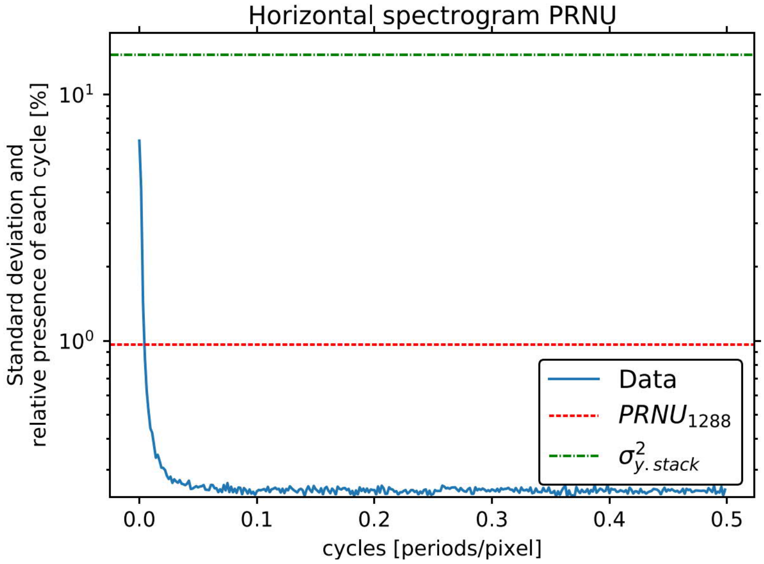

b

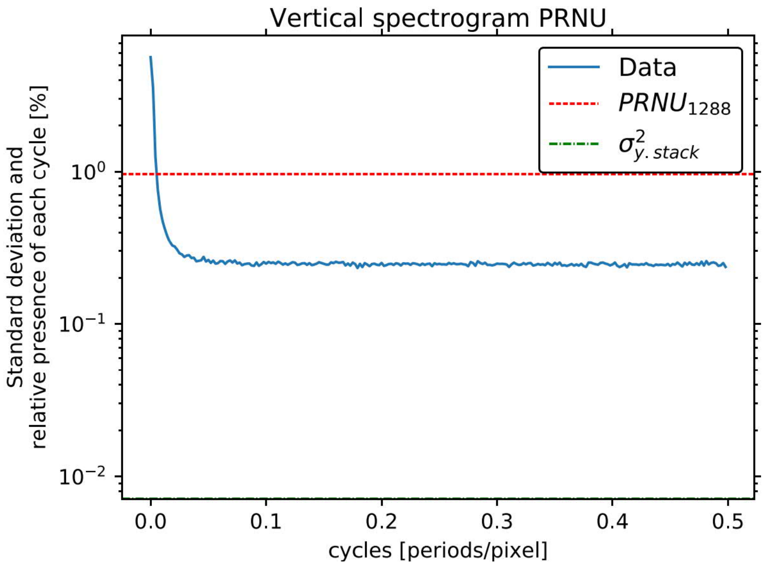

Figure 11: *Example for spectrograms of the photoresponse:* ***a*** *horizontal spectrogram* ***b*** *vertical spectrogram.*

image $\langle \boldsymbol{y}_{50} \rangle - \langle \boldsymbol{y}_{\text{dark}} \rangle$ defined in Section 4.2 without applying any corrections such as high-pass filtering.

The ranges of the profiles are set as follows:

DSNU profiles Take 0.9 times average of minimum line as lower limit and 1.1 times of average of maximum line as upper limit,

PRNU profiles Take 0.9 times average of mean value as lower limit and 1.1 times of average of mean value as upper limit. For PRNU profiles measured with a lens/camera combination take a range from zero to the maximum.

Label axes of both DSNU and PRNU profiles with units DN.

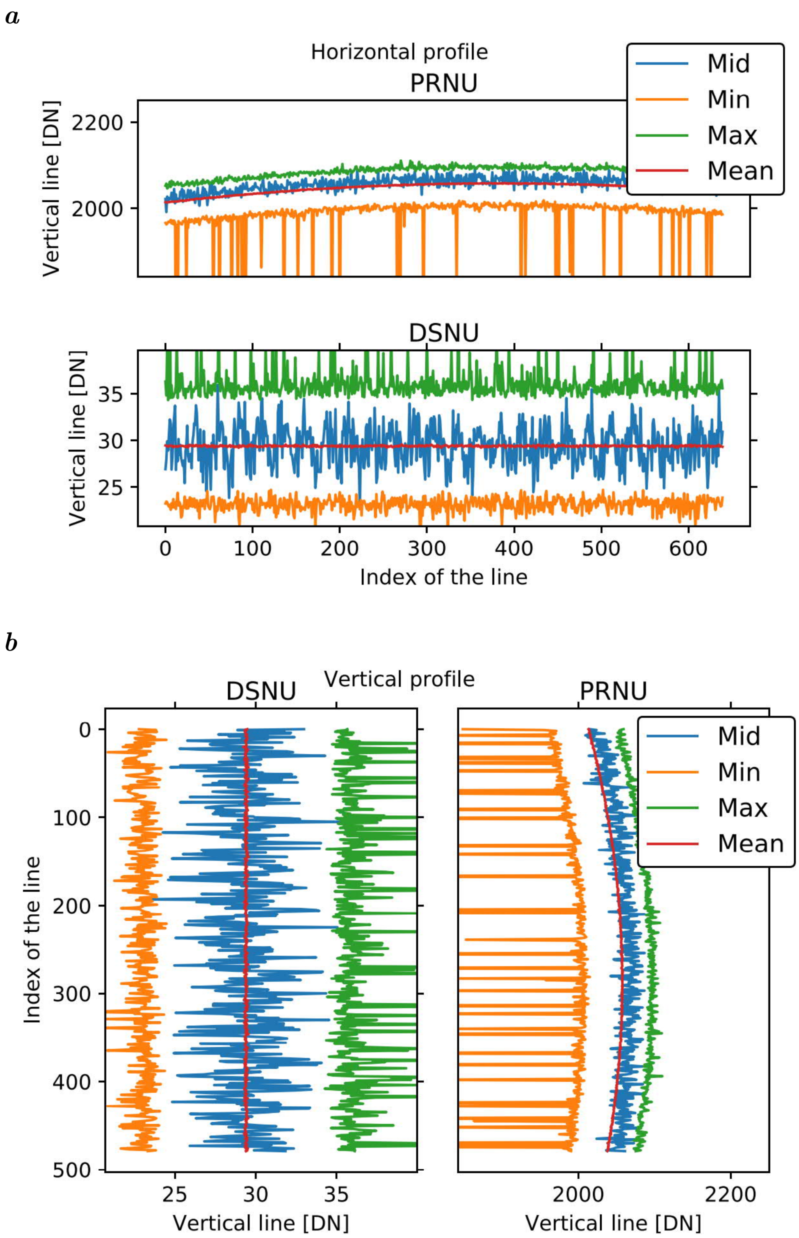

Figure 12: *Example for profile images:* ***a*** *horizontal profiles* ***b*** *vertical profiles.*

8.8 Defect Pixel Characterization

The computation of the logarithmic histogram involves the following computing steps for every averaged and highpass-filtered nonuniformity image $\boldsymbol{y}$. The following procedure is suggested to obtain optimally smooth histograms. It is based on the simple fact that nonuniformity images are averaged over L integer-valued images. Therefore their values are integer multiples of $1/L$ and the optimum interval width is therefore also an integer multiple of L.

1. Compute minimum and maximum values $y_{\min}$ and $y_{\max}$ of the image $\boldsymbol{y}$.
2. Part the interval between $y_{\min}$ and $y_{\max}$ into $Q = L(y_{\max} - y_{\min})/I + 1$ bins of equal width with the optimal bin width of I/L. Choose an appropriate $(I = 1, 2, 3, \ldots)$ so that the number of bins is lower than or equal to 256. This condition is met by

$$I = \text{floor}\left[\frac{L(y_{\max} - y_{\min})}{256}\right] + 1. \tag{64}$$

3. Compute a histogram with all values of the image using these bins. The bin q to be

incremented for a value y is

$$q = \text{floor}\left[\frac{L(y - y_{\min})}{I}\right]. \tag{65}$$

In this way the Q bins of the histogram (indices from 0 to $Q-1$) cover values from $y_{\min}$ to $y_{\max} + (I-1)/L$
The values of the center of the bins as a deviation from the mean value are given as:

$$y[q] = y_{\min} + \frac{I-1}{2L} + q\frac{I}{L}. \tag{66}$$

4. Draw the histogram in a semilogarithmic plot. Use an x-axis with the values of the bins relative to the mean value. The y axis must start below 1 so that single outlying pixels can be observed.
5. Add the normal probability density distribution corresponding to the non-white variance s_{nw}^2 as a dashed line to the graph obtained for an $M \times N$ image with an interval width I/L:

$$p_{\text{normal}}[q] = \frac{I}{L} \cdot \frac{NM}{\sqrt{2\pi}\, s_{nw}} \cdot \exp\left(-\frac{y[q]^2}{2s_{nw}^2}\right). \tag{67}$$

The accumulated logarithmic histogram gives the probability distribution (integral of the probability density function) of the absolute deviation from the mean value. Thus the accumulated logarithmic histogram gives the number of pixels that show at least a certain absolute deviation from the mean in relation to the absolute deviation. The computation involves the following steps:

1. Subtract the mean from the nonuniformity image $\boldsymbol{y}$ and take the absolute value:

$$\boldsymbol{y}' = |\boldsymbol{y} - \mu_y| \tag{68}$$

2. Compute the maximum value $y'_{\max}$ of $\boldsymbol{y}'$; the minimum is zero. The rest of the computation is equivalent to the computation of the non-accumulated histograms of above if $y_{\min}$ is replaced by zero and $y_{\max}$ by $y'_{\max}$.
3. Part the interval between 0 and $y'_{\max}$ into $Q = L\, y'_{\max}/I + 1$ bins of equal width with the optimal bin width of I/L. Choose an appropriate $(I = 1, 2, 3, \ldots)$ so that the number of bins is lower than or equal to 256. This condition is met by

$$I = \text{floor}\left[\frac{L\, y'_{\max}}{256}\right] + 1. \tag{69}$$

4. Compute a histogram with all values of the image using these bins. The bin q to be incremented for a value y is

$$q = \text{floor}\left(Ly'/I\right). \tag{70}$$

The values of the center of the bins as a deviation from the mean value are given as:

$$y'[q] = \frac{I-1}{2L} + q\frac{I}{L}. \tag{71}$$

5. Accumulate the histogram. If $h[q']$ are the Q values of the histogram, then the values of the accumulated histogram $H[q]$ are:

$$H[q] = \sum_{q'=q}^{Q} h[q']. \tag{72}$$

6. Draw the accumulated histogram $H[q]$ as a function of $y'[q]$ in a semilogarithmic plot. Use a x-axis with the values of the bins relative to the mean value. The y axis must start below 1 so that single outlying pixels can be observed.

Logarithmic histograms and accumulated logarithmic histograms are computed and drawn for both the DSNU and the PRNU. This gives four graphs in total as shown in Figs. 13 and 14.

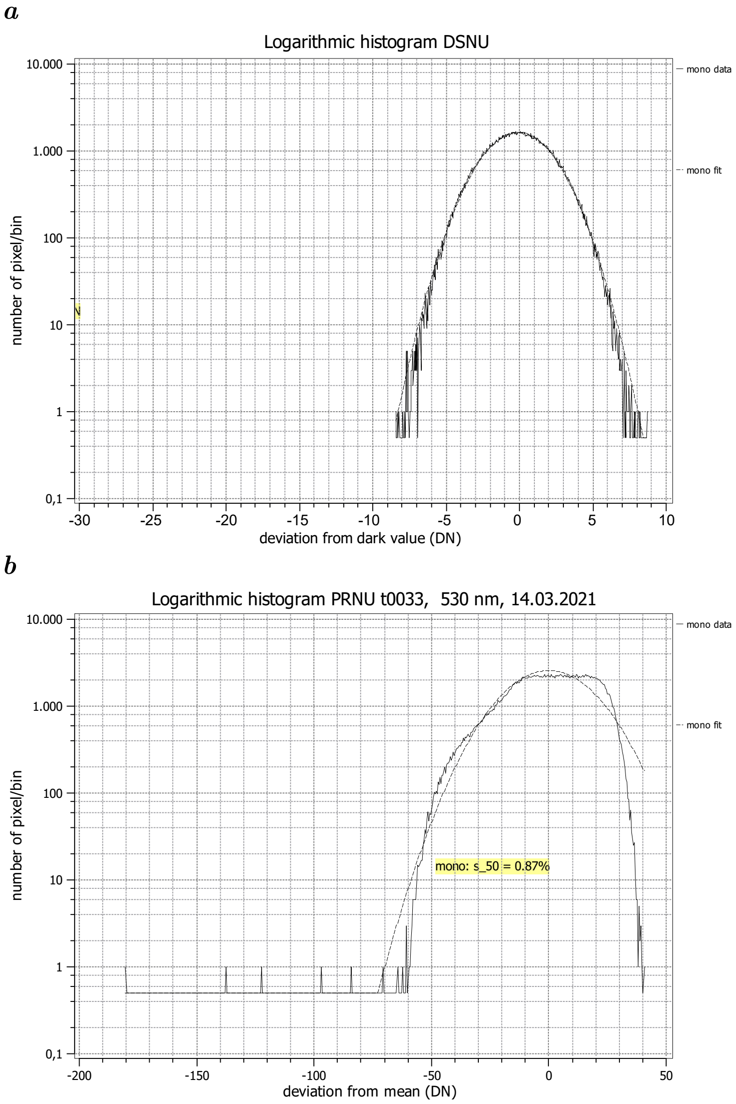

Figure 13: *Example for logarithmic histograms for **a** dark signal nonuniformity (DSNU), **b** photoresponse nonuniformity (PRNU). The dashed line is the model normal probability density distribution with the non-white standard deviation s_{nw} according to Eq. (67).*

a

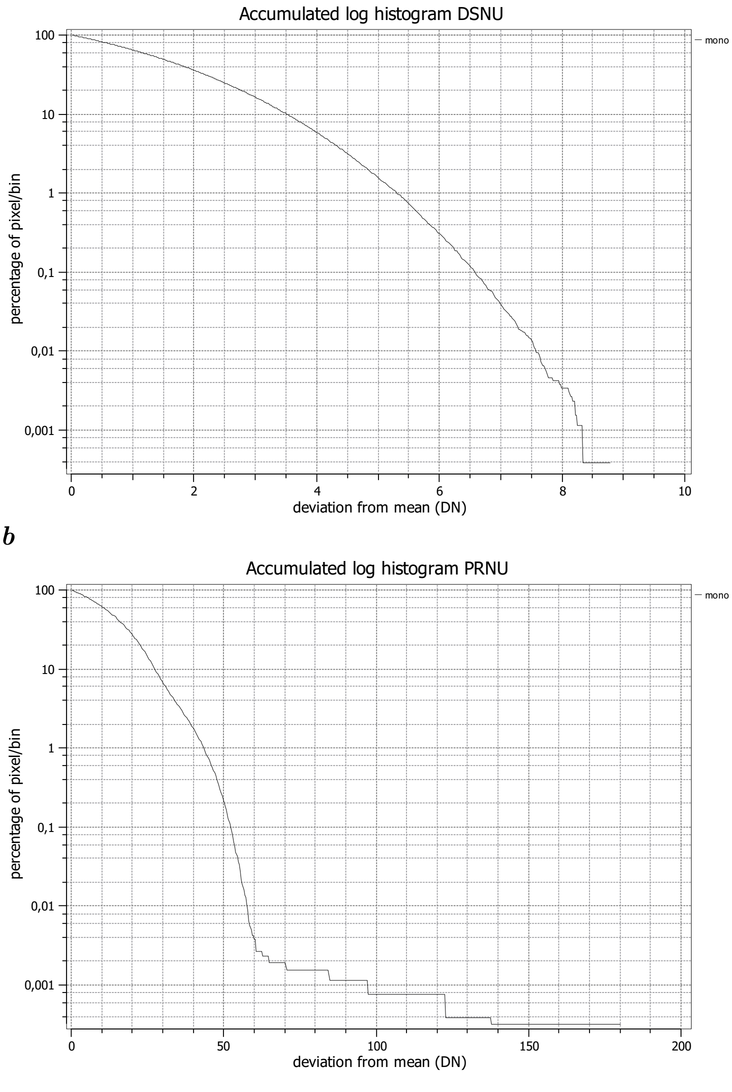

Figure 14: *Example for accumulated logarithmic histograms for* ***a*** *dark signal nonuniformity (DSNU),* ***b*** *photoresponse nonuniformity (PRNU).*

9 Methods for Spectral Sensitivity

9.1 Spectral Light Source Setup

The measurement of the spectral dependence of the quantum efficiency requires a separate experimental setup with a light source that can be scanned over a certain wavelength range. This apparatus includes either a monochromator with a broadband light source or a light source that can be switched between different wavelengths by any other means. Use an appropriate optical setup to ensure that the light source has the same geometrical properties as detailed in Section 6.1. This means that a light source with a diameter D must evenly illuminate the sensor array or calibration photodiode placed at a distance $d = 8D$ with a diameter $D' \leq D$. A different aperture d/D can be used and must be reported. It is advantageous to set up the whole system in such a way that the photon irradiance is about the same for all wavelengths.

Spectroscopic measurements are quite demanding. It might not be possible to irradiate the whole sensor evenly. Therefore only a section of the sensor may be used for the spectroscopic measurements.

For the general model it is not possible to measure absolute quantum efficiencies. It is only possible to measure the quenatum efficiency relative to the selected reference wavelength λ_{ref} which is used for a sensor or a channel of a sensor.

9.2 Measuring Conditions

This section summarizes the measuring conditions.

Sensor area. Specify the fraction of the sensor area used (all, half, ...).

Operation point. The operation point must be the same as for all other measurements.

Bandwidth. The FWHM (full width at half maximum) bandwidth of the light source shall be less than 10 nm. If it is technically not feasible to work with such narrow FWHM, the FWHM bandwidth can be enlarged to values up to 50 nm. The FWHM used for the measurement must be reported. Please note that if you use a FWHM larger than 10 nm it will not be possible to evaluate the color rendition of a color sensor, e. g., according to the ISO 13655 and CIE 15.2. Some image sensors show significant oscillations in the quantum efficiency as a function of the wavelength of the light (Fig. 15). If such oscillations occur, the peak positions vary from sensor to sensor. Therefore it is allowed to smooth, provided that the filter procedure is described including the width of the filter.

Wavelength range. The scanned wavelength range should cover all wavelength to which the sensor responds. Normally, this includes a wavelength range from at least 350 nm to 1100 nm. For UV sensitive sensors the wavelength range must be extended to correspondingly shorter wavelengths, typically down to 200 nm. If technically feasible, the number of measuring points must be chosen in such a way that the whole wavelength range is covered without gaps. This implies that the distance between neighboring wavelengths is smaller than or equal to the 2 FWHM.

Signal range. An exposure time should be set to a value so that sufficiently large signals are obtained for all wavelengths. If the radiance of the light source shows large variations for different wavelengths, this could require more than one spectral scan with different exposure times. Before and after each wavelength sweep and for every exposure time used, a dark image must be taken.

9.3 Calibration

The experimental setup is calibrated in the same way as the monochromatic setup (Section 6.4). The image sensor is replaced by a calibrated photodiode for these measurements. From the measured irradiance at the sensor surface, the number of photons $\mu_p(\lambda)$ collected during the exposure time are computed using Eq. (3).

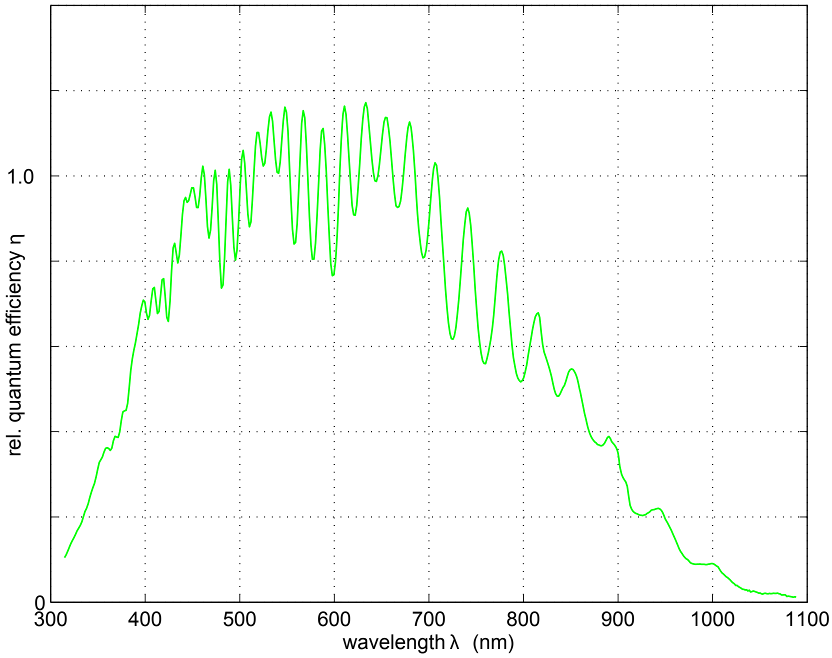

Figure 15: *Example for a spectroscopic measurement of the quantum efficiency in a range from 300–1100 nm with a FWHM of 10 nm relative to the value at a wavelength of 570 nm, no smoothing must be applied.*

9.4 Evaluation

The measured wavelength dependent quantum efficiency is averaged over all pixels of the sensor or the selected sensor area.

The evaluation procedure contains the following steps for every chosen wavelength λ. It requires a cubic B-spline regression to the inverse characteristic curve measured for the reference wavelength

$$\mu_p = R^{-1}(\mu_y - \mu_{y.\text{dark}}) \tag{73}$$

and the quantum exposure for each wavelength $\mu_p(\lambda)$:

1. Compute the mean spectral gray value $\mu_y(\lambda)$.
2. Convert this value back into the input signal using the regression of the inverse characteristic curve $R^{-1}(\mu_y - \mu_{y.\text{dark}})$ at the reference wavelength in order to linearize the signal.
3. Then the quantum efficiency relative to the quantum efficiency of the reference wavelength is given by

$$\frac{\eta(\lambda)}{\eta(\lambda_{\text{ref}})} = \frac{R^{-1}(\mu_y(\lambda) - \mu_{y.\text{dark}})}{R^{-1}(\mu_y(\lambda_{\text{ref}}) - \mu_{y.\text{dark}})} \cdot \frac{\mu_p(\lambda)}{\mu_p(\lambda_{\text{ref}})}. \tag{74}$$

An example curve is shown in Fig. 15.

10 Publishing the Results

This section describes the basic information which must be published for each camera and precedes the EMVA 1288 data.

10.1 Basic Information

Item	Description
Vendor	Name
Model	Name
Type of data presented[1]	Single; typical; guaranteed; guaranteed over life time
Sensor type	CCD, CMOS, CID, ...
Sensor diagonal	in [mm] (Sensor length in the case of line sensors)
Lens category	Indication of lens category required [inch]
Resolution	Resolution of the sensor's active area: width x height in [pixels]
Pixel size	width x height in [μm]
CCD only	
Readout type	progressive scan or interlaced
Transfer type	interline transfer, frame transfer, full frame transfer, frame interline transfer
CMOS only	
Shutter type	Global: all pixels start exposing and stop exposing at the same time. Rolling: exposure starts line by line with a slight delay between line starts; the exposure time for each line is the same. Other: defined in the datasheet.
Overlap capabilities	Overlapping: readout of frame n and exposure of frame n+1 can happen at the same time. Non-overlapping: readout of frame n and exposure of frame n+1 can only happen sequentially. Other: defined in the datasheet.
Maximum readout rate	number of frames per second (or lines per second for line sensors) at the given operation point (no change of settings permitted)
Dark current compensation	Specify whether camera has dark current compensation
Interface type	Analog[2], any of the interface standards (GigE, USB Vision, CoaxPress, ...) or proprietary
Operation point(s)	Describe operation points used for EMVA 1288 measurements (including gain, offset, maximum exposure time, mode of camera, ...). Must include all parameter so that everybody reading the datasheet can repeat the measurements. Parameters not given are assumed to be factory default.
EMVA 1288	Specify which test equipment, which release of the EMVA 1288 standard was used and which optional EMVA 1288 data have been measured

[1]Specify definition used for typical data, e. g., number of samples, sample selection. The type of data may vary for different parameters, e. g., guaranteed specification for most of the parameters and typical data for some measurements not easily done in production. It then has to be clearly indicated which data is of what nature.

[2] Specify frame grabber used with analog camera

10.2 The EMVA 1288 Datasheet

The data sheet is structured in the following way:

Optional cover page Free for anything. Typical first page from companies (key features, description, picture, etc). Any layout is possible. If present, the first page must contain the EMVA1288 logo.

Table 2: *List of all EMVA 1288 parameters*

Type of measurement	Reference
Quantum efficiency η	N/A (cannot be measured)
Gain K	N/A (cannot be measured)
Gain $1/K$	N/A (cannot be measured)
Dark noise	in units DN
	in units p
Signal to noise ratio $\mathrm{SNR}_{\mathrm{p.max}}$	as ratio
	in units dB
$\mathrm{SNR}^{-1}_{\mathrm{p.max}}$	in %
Absolute sensitivity threshold	in number of photons
	in number of photons per $\mu\mathrm{m}^2$
Saturation capacity	in number of photons
	in number of photons per $\mu\mathrm{m}^2$
Dynamic range (DR)	as ratio
	in units dB
DSNU_{1288}	in units p
$\mathrm{DSNU}_{1288.\mathrm{row}}$	in units p
$\mathrm{DSNU}_{1288\mathrm{col}}$	in units p
$\mathrm{DSNU}_{1288.\mathrm{pix}}$	in units p
PRNU_{1288}	in %
$\mathrm{PRNU}_{1288.\mathrm{row}}$	in %
$\mathrm{PRNU}_{1288.\mathrm{col}}$	in %
$\mathrm{PRNU}_{1288.\mathrm{pix}}$	in %
Non-linearity error LE	if linear in %, otherwise describe type of nonlinearity: multilinear, logarithmic, ...
Dark current from mean	in units p/s
Dark current from variance	in units p/s

General One or more pages describing the test equipment used, the version of the EMVA 1288 standard used, the basic camera parameters and a summary of the operation points for which measurements are provided (see first page of attached document). If spectrometric measurements are performed, a graph with the wavelength dependency of the quantum efficiency (Fig. 15) is included. The date when the measurement was performed must be provided on request.

Summary page for each operating point Each page is a summary of the results for one of the operating points (see second page of attached document). The summary page contains a description of the operating point, a graph with the characteristic curve (Fig. 5), a graph with the SNR curve (Fig. 7) and a one-column table with all quantities according to Table 2, which are detailed in Sections 6–9. The header contains the EMVA 1288 logo on the left and the company logo on the right.

Detailed results for each operating point For each operating point more specific details about the test conditions, large size plots, and for each plot a table with the extracted data.

A template of the summary data sheet is published together with this release in a separate document. It clearly specifies which graphs and camera parameter must be placed where in the data sheet. It also details all the axes labeling of the graphs.

A Bibliography

[1] Darmont, A.: High Dynamic Range Imaging: Sensors and Architectures, SPIE, 2 edn., doi: 10.1117/3.2512264, 2019.

[2] Darmont, A., Chahiba, J., Lemaitre, J. F., Pirson, M., and Dethier, D.: Implementing and using the EMVA1288 standard, in: Sensors, Cameras, and Systems for Industrial/Scientific Applications XIII, edited by Widenhorn, R., Nguyen, V., and Dupret, A., vol. 8298 of *Proc. SPIE*, p. 82980H, doi: 10.1117/12.905874, 2012.

[3] Denvir, D. J. and Conroy, E.: Electron multiplying CCDs, in: Optical Metrology, Imaging, and Machine Vision, edited by Shearer, A., Murtagh, F. D., Mahon, J., and Whelan, P. F., vol. 4877 of *SPIE Proc.*, pp. 55–68, 2003.

[4] DeWeert, M. J., Cole, J. B., Sparks, A. W., and Acker, A.: Photon transfer methods and results for electron multiplication CCDs, in: Applications of Digital Image Processing XXVII, edited by Tescher, A. G., vol. 5558 of *SPIE Proc.*, pp. 248–259, 2004.

[5] Dierks, F.: Sensitivity and Image Quality of Digital Cameras, Tech. rep., Basler AG, 2004.

[6] Dittrich, P.-G., Bichra, M., Pfützenreuter, C., Rosenberger, M., and Notni, G.: Measurement principle and arrangement for the determination of spectral channel-specific angle dependencies for multispectral resolving filter-on-chip CMOS cameras, in: Photonics and Education in Measurement Science 2019, edited by Rosenberger, M., Dittrich, P.-G., and Zagar, B., vol. 11144, pp. 180–190, International Society for Optics and Photonics, SPIE, doi: 10.1117/12.2527871, 2019.

[7] Dittrich, P.-G., Bichra, M., Stiehler, D., Pfützenreuter, C., Radtke, L., Rosenberger, M., and Notni, G.: Extended characterization of multispectral resolving filter-on-chip snapshot-mosaic CMOS cameras, in: Algorithms, Technologies, and Applications for Multispectral and Hyperspectral Imagery XXV, edited by Velez-Reyes, M. and Messinger, D. W., vol. 10986, pp. 140–150, International Society for Optics and Photonics, SPIE, doi: 10.1117/12.2518842, 2019.

[8] Dittrich, P.-G., Rosenberger, M., and Notni, G.: Measurement, comparison, and evaluation of spectral sensitivity curves from different multispectral resolving snapshot-mosaic cameras, in: Algorithms, Technologies, and Applications for Multispectral and Hyperspectral Imagery XXVI, edited by Velez-Reyes, M. and Messinger, D. W., vol. 11392, International Society for Optics and Photonics, SPIE, doi: 10.1117/12.2564690, 2020.

[9] EMVA 1288 Working Group: EMVA Standard 1288 - Standard for Characterization of Image Sensors and Cameras, Release 3.1, open standard, European Machine Vision Association, doi: 10.5281/zenodo.235942, 2016.

[10] Holst, G. C. and Lomheim, T. S.: CMOS/CCD Sensors and Camera Systems, SPIE Press, Bellingham, Washington, USA, 2 edn., 2011.

[11] Janesick, J., Klaasen, K., and Elliott, T.: CCD charge collection efficiency and the photon transfer technique, in: Solid State Imaging Arrays, edited by Dereniak, E. L. and Prettyjohns, K. N., vol. 570, pp. 7–19, Proc. SPIE, doi: 10.1117/12.950297, 1985.

[12] Janesick, J. R.: Scientific Charge-Coupled Devices, SPIE, Bellingham, WA, doi: 10.1117/3.374903, 2001.

[13] Jähne, B.: Digital Image Processing, Springer, Berlin, 6 edn., doi: 10.1007/3-540-27563-0, 2005.

[14] Jähne, B.: Release 4 of the EMVA 1288 standard: adaption and extension to modern image sensors, in: Forum Bildverarbeitung, edited by Heizmann, M. and Längle, T., pp. 13–24, KIT Scientific Publishing, doi: 10.5445/KSP/1000124383, 2020.

[15] Labsphere: A Guide to Integrating Sphere Theory and Applications, technical guide, see http://www.labsphere.com/, 2003.

[16] Labsphere: Integrating Sphere Uniform Light Source Applications, technical guide, see http://www.labsphere.com/, 2003.

[17] Papoulis, A.: Probability, Random Variables and Stochastic Processes, McGraw-Hill, 3 edn., 1991.

[18] Radtke, L., Graf-Batuchtin, I., Rosenberger, M., and Notni, G.: Adaptive test bench for characterizing image processing sensors, in: Image Sensing Technologies: Materials, Devices, Systems, and Applications V, vol. 10656 of *Proc. SPIE*, doi: 10.1117/12.2304874, 2018.

[19] Rebhan, D., Dittrich, P.-G., Rosenberger, M., and Notni, G.: Radiometric extension of a measurement arrangement in accordance with the EMVA 1288 standard for camera characterization in UV to NIR wavelength range, Journal of Physics: Conference Series, 1379, 012 056, doi: 10.1088/1742-6596/1379/1/012056, 2019.

[20] Rosenberger, M., Zhang, C., Votyakov, P., Preißler, M., Celestre, R., and Notni, G.: EMVA 1288 camera characterisation and the influences of radiometric camera characteristics on geometric measurements, Acta IMEKO, 5, 81–87, doi: 10.21014/acta_imeko.v5i4.356, 2016.

[21] Theuwissen, A. J. P.: Solid-State Imaging with Charge-Coupled Devices, Kluwer Academic Publishers, doi: 10.1007/0-306-47119-1, 1995.

[22] Widrow, B. and Kollar, I.: Quantization Noise — Roundoff Error in Digital Computation, Signal Processing, Control, and Communications, Cambridge Univ Press, URL www.cambridge.org/9780521886710, 2008.

B Notation

This section summarizes the used notation in two tables. The first table describes all quantities used, the second table, the meaning of indices that are used with various quantities. With this split in the description, the notation tables are much shorter.

Quantity	Units	Description
A	μm^2	Area of a sensor element (pixel)
c	m/s	Velocity of light
d	mm	Distance of sensor plane to opening (aperture) of light source
D	mm	Diameter of opening (aperture) of light source
D'	mm	Diameter of image sensor
DSNU_{1288}	DN	Dark signal nonuniformity
DR	1, dB, bits	Dynamic range
E	W/m^2, Photons/(s pixel)	Irradiance and quantum irradiance at sensor plane
h	Js	Planck constant
H	Ws/m^2, Photons/pixel	Radiant and quantum exposure at sensor plane
k	m^{-1}	wave number
K	DN/e$^-$	Overall system gain of a digital camera
PRNU_{1288}	%	Photo response nonuniformity
SNR	1, dB, bits	Signal-to-noise ratio
$\boldsymbol{P}$	—	Power spectrum
R	DN/p	Responsivity (slope characteristic curve)
s	—	*spatial* standard deviation of the quantity put into the index
s^2	—	*spatial* variance of the quantity put into the index
$\boldsymbol{s}$	DN	Digital image sequence
t_{exp}	s	Exposure time
y	DN	Digital gray value
$\boldsymbol{y}$	DN	2-D digital image
η	1	Total quantum efficiency, def. Eq. (2)
λ	nm	wavelength of light
μ	—	mean of the quantity put into the index
ν	Hz	frequency of light
σ	—	*temporal* standard deviation of the quantity put into the index
σ^2	—	*temporal* variance of the quantity put into the index

Index	Units	Description
d	e^-	relates to dark signal in units of e^-
dark	DN	relates to dark signal in units of DN
e	—	relates to number of electrons
min	—	relates to absolute sensitivity threshold
p	—	relates to number of photons
q	—	relates to quantization noise
sat	—	relates to saturation of the sensor
stack	—	relates to an image sequence (stack of images)
y	—	relates to a digital gray value
[l]	—	selection of image number l from an image sequence with L images, l runs from 0 to $L-1$
[m]	—	selection of a row in an image, m runs from 0 to $M-1$
[n]	—	selection of a column in an image, n runs from 0 to $N-1$

C Limit for Minimal Temporal Standard Deviation; Introduction of Quantization Noise

In the previous releases of the standard, quantization noise was neglected in the linear camera model. This led to a more complicated measuring procedure with low-resolution digitalization, i. e., 8 bit cameras. The problem resulted from the fact that the standard deviation of the temporal noise in the dark image may become smaller than the quantization interval.

Versions 1 and 2 of the EMVA 1288 standard therefore recommended:

"The gain setting of the camera is as small as possible but large enough to ensure that in darkness

$$K\sigma_d \geq 1$$

holds true (Otherwise, the quantization noise will spoil the measurement.)"

It turns out that this limit is too cautious [22]. Monte-Carlo simulations were performed to check how accurate the mean and the variance can be estimated as a function of standard deviation σ_y in units DN. For the simulations 201 mean gray values equally distributed between 0 and 1 were taken and zero-mean normally distributed noise was added to the values. The estimated mean and variances were averaged over 900 000 realizations of each value. Finally, the deviations in the estimations were averaged over all 201 values.

The results are shown in the range $[0.3, 1]$ for σ_y in Fig. 16. The mean gray value can be estimated with a maximum error of less than 0.014 DN even for standard deviations as low as 0.4 DN (Fig. 16b). The estimate of the standard deviation is biased by the additional standard deviation of the quantization, $\sigma_q = \sqrt{1/12}$. However, if the estimate of the standard deviation is corrected for the additional effect of the standard deviation of the quantization error (unbiased estimation)

$$\sigma_y^2 = \sigma_{\text{est}}^2 - \sigma_q^2 = \sigma_{\text{est}}^2 - 1/12, \tag{75}$$

the maximum error of the estimate remains below 0.04 DN even for standard deviations as low as 0.4 DN. The variation in the estimation of the standard deviation comes from the different positions of the mean in the $[0, 1]$ interval. If it is close the edge of the interval, the values flip often either to the higher or lower value, resulting in a higher standard deviation. If the mean is in the middle of the interval this happens less frequently, so that the standard deviation is lower.

According to Eq. (18), the temporal noise is measured using the difference of two images. Therefore the temporal standard deviation of the difference image must be larger than 0.40 DN ... In conclusion, the variance $\sigma_{y.\text{dark}}^2$ must be larger than 0.24 DN^2. Subtracting the quantization noise variance $\sigma_q^2 = 1/12\,\text{DN}^2$, this results in a minimal detectable temporal standard deviation of 0.40 DN. If the measured temporal variance is smaller than 0.24 DN^2, two things can be stated:

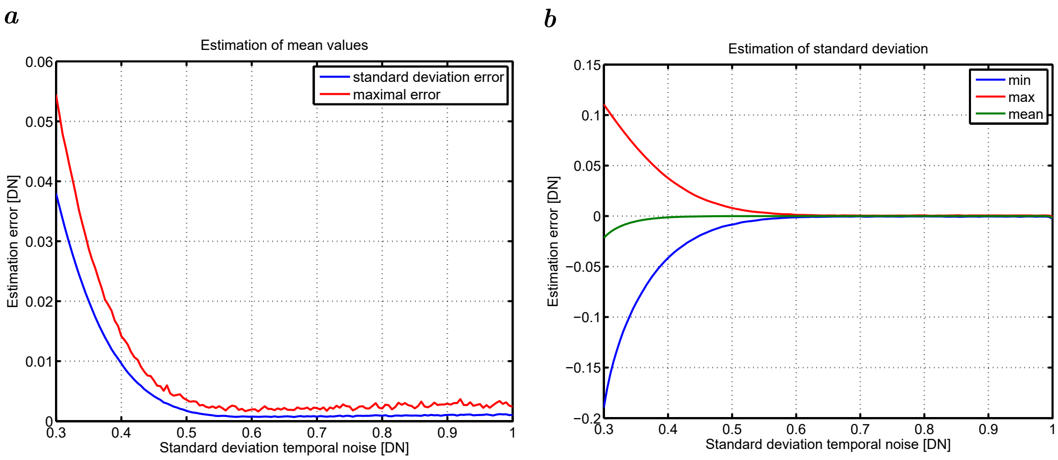

Figure 16: *Results from Monte Carlo simulations for the estimation of* ***a*** *the mean value and* ***b*** *the standard deviation of the digital gray value as a function of the standard deviation in units of digital numbers [DN] in the range between 0 and 1.*

1. The dynamic range is limited by the quantization noise (and the maximum possible but not determinable temporal noise to $\mu_{y.\text{sat}}/0.49$.
2. The standard deviation of the dark noise in units e^- can be estimated to $\sigma_d < 0.40/K$.

The correction of the temporal noise by the quantization noise, which is possible down to a measured temporal noise variance of 0.24, expands the measurable dynamic range of a camera by a factor of about 2 over the condition of release A2.01. For a 8-bit camera, the maximum and measurable dynamic range is $255/0.49 \approx 500$.

D Differences between Release 4.0 Linear and General

This section summarizes the differences between Release 4.0 Linear and General. The essential point is that the same measurements are performed but that they are analyzed in a different way.

D.1 Differences in Setup of Measurements and Measuring Conditions

Generally there are no differences in the measurements performed with one small but important exception. In order to measure the slope of the characteristic curve close to the dark value accurately enough, the exposure steps should also include enough values a low signal to noise ratios in the range of one. This requires to extend the exposure steps over a significantly wider range of exposures. Applying this does not harm the measurements for linear sensors as well. Therefore it makes sense to extend the number of exposure steps over the recommended minimum number of 50 steps for *all* measurements, independently which model is used for evaluation.

D.2 Differences in the Evaluation

1. The photon transfer curve makes no sense and is not used. Therefore in the summary sheet, the photon transfer curve is replaced by the characteristic curve. With this curve, the type of non-linearity becomes immediately visible
2. For non-linear characteristic curves it is important to distinguish between input SNR_p and output SNR_y. The really important quantity is the input SNR_p. Therefore all quantities measured at the output are transformed to the input signal by using the slope of the characteristic curve and the SNR of the linear model is replaced by the input SNR_p.
3. The quantum efficieny η and the system gain K the are reported as not measurable in the summary sheet. However, the cover sheet can optionally include the measured quantum

efficiency relative to the reference wavelength chosen for all other measurements of a sensor channel.

4. No parameters in units of electrons can be reported, because the absolute quantum efficiency is not known. Therefore these quantities are reported in units of photons.

E List of Contributors and History

EMVA gratefully acknowledges the active contributions to release 4.0 of this standard by the following members of the EMVA 1288 standardization committee, given in alphabetic order:

- Allied Vision Technologies GmbH, Stadtroda, Germany
- Basler AG, Ahrensburg, Germany
- Baumer Optronic GmbH, Radeberg, Germany
- FLIR Machine Vision, Richmond, Canada
- Gpixel nv, Antwerpen, Belgium
- HCI, Heidelberg University, Heidelberg, Germany
- Image Engineering GmbH & Co. KG, Köln, Germany
- JAI A/S, Copenhagen, Denmark
- Kaya Instruments, Nesher, Israel
- Labsphere, Inc., North Sutton, NH, USA
- LOOKLONG Imaging, Xi'an, China
- MATRIX VISION GmbH, Oppenweiler, Germany
- Matrox Electronic Systems Ltd., Dorval, Quebec, Canada
- PCO AG, Kelheim, Germany
- ON Semiconductor, Phoenix, Arizona, United States
- STEMMER IMAGING AG, Puchheim, Germany
- Technical University Ilmenau, Germany

The history of the EMVA 1288 dates back to 2004. The first meeting took place on February 2004 in Frankfurt, Germany. Among the initiators were Martin Wäny (Awaiba) and Fritz Dierks (Basler AG). Other major initial contributions came from Albert Theuwissen (then Dalsa) and Emil Ott (PCO AG). The founding chair was Martin Wäny. Since 2008 the EMVA 1288 committee is chaired by Bernd Jähne (HCI, Heidelberg University).

A table of all releases of the EMVA standard 1288 concludes this document.

Date	Version	Document
August 2005	Release A1.00	`https://doi.org/10.5281/zenodo.3951558`
September 2006	Release A1.03	`https://doi.org/10.5281/zenodo.1402249`
August 2007	Release A2.01	`https://doi.org/10.5281/zenodo.1402251`
November 19, 2010	Release 3.0	`https://doi.org/10.5281/zenodo.10696`
December 30, 2016	Release 3.1	`https://doi.org/10.5281/zenodo.235942`
December 25, 2017	Chinese translation	`https://doi.org/10.5281/zenodo.3541785`
June 16, 2021	Release 4.0 Linear	**Available here**
June 16, 2021	Release 4.0 General	**This document**

F Template of Summary Data Sheet

See appended page.

Summary Sheet for Operation Point 1 at a Wavelength of 530 nm

Type of data	Single	Gain, black-level	0.0 dB, 5 DN
Exposure control	By irradiance	Environmental temperature	20.0°C
Exposure time	1.00 ms	Camera body temperature	29.0°C
Frame rate	100.0 Hz	Internal temperature(s)	—
Data transfer mode	Mono 12	Wavelength, centr., FWHM	530 nm, 30.0 nm

Characteristic Curve

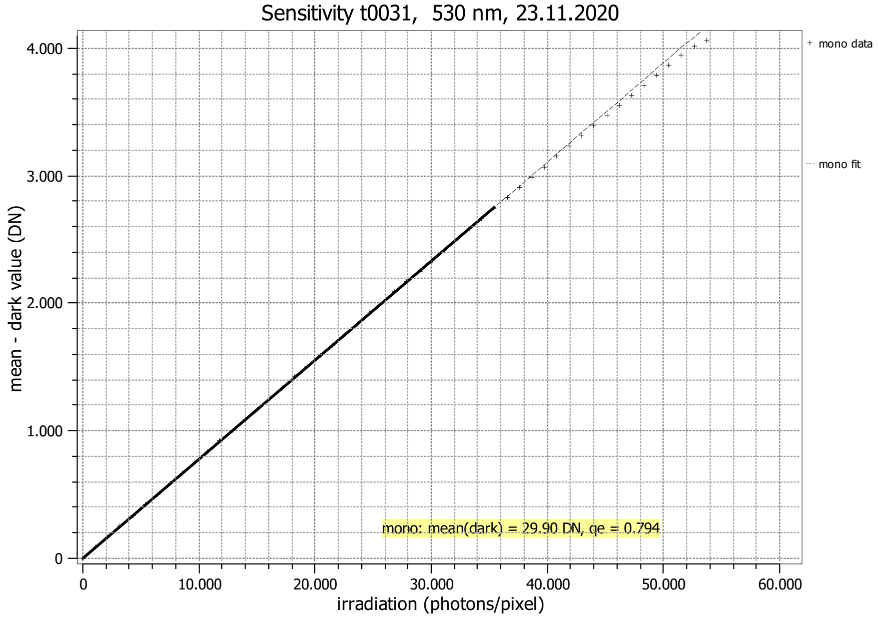

Signal-to-Noise Ratio

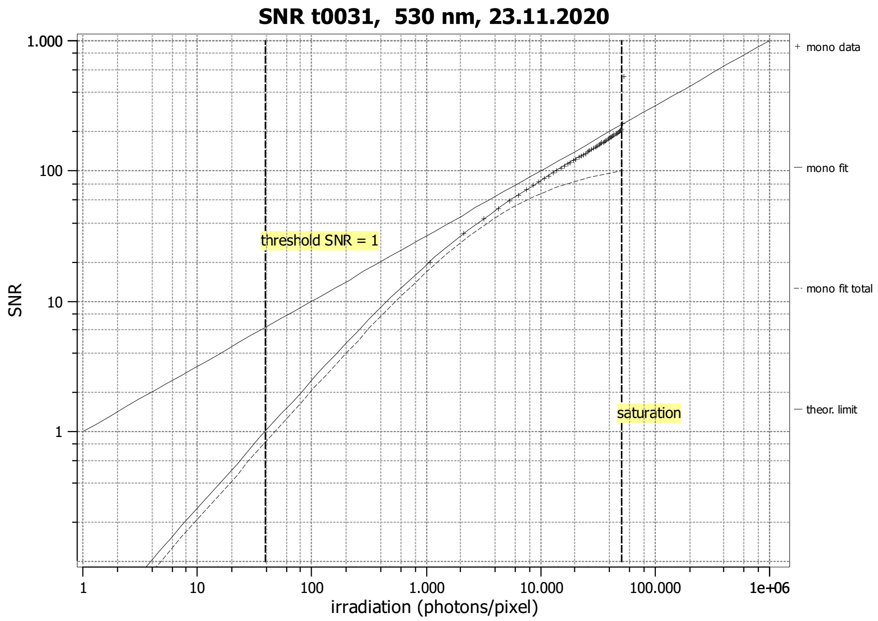

Quantum efficiency	
η	N/A
Overall system gain	
K	N/A
$1/K$	N/A
Temporal dark noise	
σ_d	30.8 p
$\sigma_{y.\text{dark}}$	3.03 DN
Signal-to-noise ratio	
SNR_{max}	202
	46.1 dB
$1/\text{SNR}_{\text{max}}$	0.49 %
Absolute sensitivity threshold	
$\mu_{p.\text{min}}$	39.6 p
$\mu_{p.\text{min.area}}$	1.15 p/μm^2
Saturation capacity	
$\mu_{p.\text{sat}}$	51548 p
$\mu_{p.\text{sat.area}}$	1501 p/μm^2
Dynamic range	
DR	1303
	62.3 dB
Spatial nonuniformities	
DSNU_{1288}	21.7 p
$\text{DSNU}_{1288.\text{col}}$	11.2 p
$\text{DSNU}_{1288.\text{row}}$	2.3 p
$\text{DSNU}_{1288.\text{pix}}$	18.4 p
PRNU_{1288}	0.87%
$\text{PRNU}_{1288.\text{col}}$	0.40%
$\text{PRNU}_{1288.\text{row}}$	0.21%
$\text{PRNU}_{1288.\text{pix}}$	0.74%
Linearity error	
LE	0.36%
Dark current	
$\mu_{c.\text{mean}}$	5.1 ± 0.2 p/s
$\mu_{c.\text{var}}$	5.2 ± 0.4 p/s